UNCLASSIFIED

AD NUMBER

AD850929

NEW LIMITATION CHANGE

TO

Approved for public release, distribution unlimited

FROM

Distribution authorized to U.S. Gov't. agencies and their contractors; Administrative/Operational Use; Feb 1969. Other requests shall be referred to Air Force Materials Lab., Metals and Ceramics Div. [MAM], Wright-Patterson AFB, OH 45433.

AUTHORITY

Air Force Materials Lab ltr, 12 Jan 1972

THIS PAGE IS UNCLASSIFIED

AFML-TR-68-231

AD850929

INVESTIGATION OF ELASTICITY AND STRENGTH OF CERAMICS SUBJECTED TO TENSILE AND COMPRESSIVE LOADS

R. SEDLACEK

Stanford Research Institute

Menlo Park, California 94025

TECHNICAL REPORT AFML-TR-68-231

APR 23 1969

FEBRUARY 1969

This document is subject to special export controls and each transmittal to foreign governments or foreign nationals may be made only with prior approval of the Metals and Ceramics Division (MAM), Air Force Materials Laboratory, Wright-Patterson Air Force Base, Ohio 45433.

AIR FORCE MATERIALS LABORATORY
AIR FORCE SYSTEMS COMMAND
WRIGHT-PATTERSON AIR FORCE BASE, OHIO 45433

84

NOTICE

When Government drawings, specifications, or other data are used for any purpose other than in connection with a definitely related Government procurement operation, the United States Government thereby incurs no responsibility nor any obligation whatsoever; and the fact that the Government may have formulated, furnished, or in any way supplied the said drawings, specifications, or other data, is not to be regarded by implication or otherwise as in any manner licensing the holder or any other person or corporation, or conveying any rights or permission to manufacture, use, or sell any patented invention that may in any way be related thereto.

This document is subject to special export controls and each transmittal to foreign governments or foreign nationals may be made only with prior approval of the Metals and Ceramics Division (MAM), Air Force Materials Laboratory, Wright-Patterson Air Force Base, Ohio 45433.

Distribution of this report is limited for protection of technical know-how relating to technology restricted by Export Control Acts.

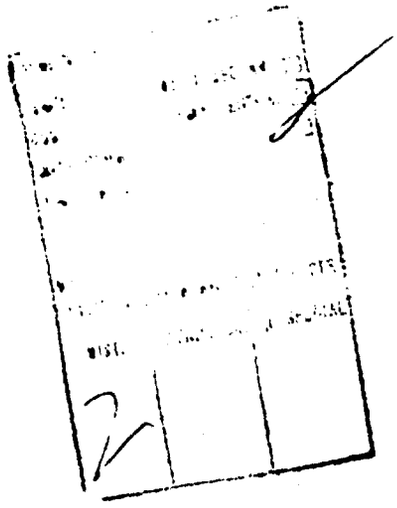

Copies of this report should not be returned unless return is required by security considerations, contractual obligations, or notice on a specific document.

500 - March 1969 - CO455 - 71-1582

INVESTIGATION OF ELASTICITY AND STRENGTH OF CERAMICS SUBJECTED TO TENSILE AND COMPRESSIVE LOADS

R. SEDLACEK

This document is subject to special export controls and each transmittal to foreign governments or foreign nationals may be made only with prior approval of the Metals and Ceramics Division (MAM), Air Force Materials Laboratory, Wright-Patterson Air Force Base, Ohio 45433.

FOREWORD

This work was performed by Stanford Research Institute under USAF Contract No AF 33(615)-5047, initiated under Project No. 7350. The program was under the administrative direction of the Air Force Materials Laboratory, Wright-Patterson Air Force Base, Ohio. Mr. G. R. Atkins was the Project Engineer.

This report covers work conducted from 15 April 1966 to 31 May 1968 under the specific direction of Rudolf Sedlacek and the general direction of F. A. Halden.

Manuscript released by the author in August 1968 for publication as a technical report.

This technical report has been reviewed and is approved.

W. J. Trapp
Chief, Strength and Dynamics Branch
Air Force Materials Laboratory

ABSTRACT

A new method of compressive testing of ceramics was perfected, and the average ultimate compressive strength of Al-995 alumina was determined to be 448,000 ± 36,000 psi at a loading rate of 10,000 psi/sec. Compressive prestressing was found to have no significant effect on the ultimate tensile strength of alumina, but extensive cyclic testing did lower the ultimate tensile strength. A statistical evaluation of test data supported these experimental results. Compressive and tensile elastic moduli and Poisson's ratios were measured. Flexural strength was found to be slightly higher than tensile strength. A theoretical analysis and experimental study were made of the effect of out-of-roundness on the nominal tensile strength of internally pressurized cylindrical test specimens. It was found that the effect of out-of-roundness which is occasionally encountered in commercially fabricated ceramic specimens is small and well within the experimental data scatter.

This abstract is subject to special export controls and each transmittal to foreign governments or foreign nationals may be made only with prior approval of the Metals and Ceramics Division (MAM), Air Force Materials Laboratory, Wright-Patterson Air Force Base, Ohio 45433

CONTENTS

ILLUSTRATIONS

TABLES

SECTION I

INTRODUCTION

A considerable research effort is currently being directed toward gaining a better understanding of the mechanical properties of ceramics, because it is apparent that the requirements of modern technology are already calling for materials capable of mechanical performance under conditions which metals and alloys cannot endure. Unfortunately, most of the existing knowledge of mechanical properties of ceramics has been generated by methods developed for the study of metals which do not take into account a basic difference between metals and ceramics, i.e., the brittleness of the latter. This omission has been most damaging in studies of the tensile strength, which is the most widely studied and important property, being the lowest and, therefore, limiting strength.

Older tensile strength data found in the literature show such discord and scatter that ceramics could never be considered for any critical structural applications in spite of other favorable characteristics of these materials. Fortunately, in the not too distant past, it became apparent to some workers in this field that the scatter of tensile strength data does not necessarily reflect an inherent materials property, but that it may be to a large extent the result of the use of improper testing methods. Since then, a considerable number of new tensile testing methods have been proposed. All of these methods essentially attempt to eliminate parasitic stresses that are superimposed on the measured primary stress during testing.

Considerable effort has been concentrated on two promising test methods: the direct pull test using gas bearings developed at the Southern Research Institute[1] and the hydraulically expanded ring test developed at Stanford Research Institute.[2] Both of these methods have been used extensively in various studies of factors influencing the tensile strength[3,4] of ceramics and have consistently yielded very reproducible results. Their

superiority has also been clearly shown in a recent survey of mechanical testing procedures for brittle materials.[5] However, these test methods have not yet been generally adopted, mainly because they require a rather sophisticated apparatus, parts of which are not commercially available.

For this reason, many studies of the mechanical properties of ceramics are still being done by the determination of tensile strength in three- or four-point bending. Obvious advantages of this method are that standard laboratory equipment (universal testing machines) can be used, loading fixtures are usually simple, and the technique is amenable to high temperature testing. On the other hand, the method has numerous disadvantages such as the existence of stress concentrations and friction at the load supports, a steep stress gradient with a minimum volume of the test specimen exposed to maximum stress, an uncertainty about the effect of specimen geometry on the observed strength, etc.

Perhaps the most severe shortcoming of the bend test is that for a given brittle material, the flexural strength values are always higher than strength data obtained in uniaxial tension on the same material. Considering the many disadvantages of the bend test, it would be illogical to assume that flexural strength values come closer to the true ultimate tensile strength of a brittle test material than values from a carefully conducted uniaxial tensile test. There is presently no generally accepted explanation to account for the discrepancies of various test methods. One possibility to reconcile the discrepancy between flexural and tensile strength data was explored in the program described in the following report.

The main objective of this program was to study possible differences between tensile and compressive elastic properties of a high alumina body and to determine how these differences (if they exist) could influence the interpretation of flexural strength data. Secondary objectives of this work were to evaluate the effect of imperfect specimen geometry on the tensile strength determined by the SRI ring test and to assess the effect of various modes of preloading on the ultimate tensile strength of alumina.

SECTION II

SUMMARY

A new method was employed and apparatus was constructed for the determination of strength and elastic properties of ceramics in compression. The method employs the same mode of loading (hydrostatic pressure) and the same specimen configuration as the SRI tensile ring test; the only difference is that in the compressive test, pressure is applied to the outside wall of the specimen. Thus a tangential compressive stress is generated whose maximum is on the inner wall of the specimen.

The average ultimate compressive strength of Al-995 alumina was found to be 448,000 ± 36,000 psi at a loading rate of 10,000 psi/sec. This value is approximately 14 times higher than the average ultimate tensile strength (31,600 ± 1100 psi) of this material at a loading rate of 3000 psi/sec.

Elastic properties in tension and compression were compared using the same test material. It was found that the values of Young's modulus are the same in tension as in compression, i.e., 53.6×10^6 psi, and no departure from linearity of the stress-strain relationship was observed.

Flexural strength data were obtained in four-point bending at the stress rate of 3000 psi/sec. The average value obtained was 36,900 ± 3000 psi. No explanation was found why the observed flexural strength is higher than strength data from the uniaxial tensile tests.

The effect of various modes of preloading on the ultimate tensile strength of alumina was also examined. Exposure to 75% of maximum compressive stress (338,000 psi) did not impair the ultimate tensile strength of the material. Similarly, ten, twenty, and forty cyclic tensile stresses on the order of 80% of the maximum tensile strength (using a frequency of 4 cps and a stress ratio of 0.14) showed no effect. However, exposure to 80 cycles, under the same conditions, resulted in considerable strength deterioration. A statistical analysis of test data supported the experimental results.

A theoretical analysis was made of the effect of ellipticity on the apparent tensile strength of nominally round cylindrical specimens stressed by internal pressure. The analysis took into account the changes in geometry of an elliptical cylinder that are incurred during pressurization, and the assumption was made that with increasing pressure, the bending stresses superimposed on the tangential tensile stresses increase until they approach a constant value when the cylinder becomes circular. Calculations made by this method showed that the magnitude of bending stresses generated by internal pressure within the wall of an elliptical specimen is a function of the size and cross-sectional rigidity of the specimen. It was calculated that the effect on measured tensile strength of a small degree of ellipticity (0.05%), which is occasionally found in ceramic specimens used in the SRI tensile ring test, is small, causing an error which is well within the range of the experimental data scatter. Photoelastic studies on elliptical specimens made of Columbia Resin CR-39 corroborated the results of the theoretical analysis. However, tensile strength measurements on Plexiglas and ATJ graphite specimens having 0% to 5% ellipticity showed a much smaller effect of out-of-roundness on measured strength than that predicted by theory. This phenomenon can be explained by the nonlinearity of the stress-strain relationship exhibited by these materials at high stress levels and low stress rates.

SECTION III

STRENGTH AND ELASTIC PROPERTIES OF AL-995 ALUMINA

1. Materials

The test material used in this study was a high-alumina commercial body, Al-995, produced by the Western Gold and Platinum Co., Belmont, California. All tensile and compressive specimens originated from the same batch of raw material and were processed as uniformly as possible. Isostatically formed hollow cylinders were bored, turned, and sliced into rings, which were fired simultaneously in a large gas-fired kiln. The "as fired" blanks were ground at the Institute by the method developed under a different contract.[6] In this method all grinding operations are performed on the same machine (Universal grinder Tschudin, Model HTG-300). The blanks are first faced so that they all have the same height and parallel faces. Then five blanks are arranged into a stack which is positioned on top of a thick-walled ceramic anchor ring. The entire assembly is heated in an oven to approximately 90°C and the stack is painted on the outside with molten Carnauba wax, which penetrates, by surface tension, between the adjacent rings. After cooling, the stack is mounted on the base of a modified drill pad whose tapered shank fits into the spindle of the workhead. The face of the drill pad has been ground *in situ* leaving in the center a protruding core 3/16 inch high that fits tightly into the inside diameter of the ceramic anchor ring. Finally, the anchor ring is firmly attached to the drill pad by a metal retaining ring. First, the entire outside of the stack is ground to the final dimension, and then the inside is finished. Since the stack of rings is removed from the drill pad only after all grinding operations have been completed, the outside and inside wall of the stack are perfectly concentric and there is no variation in wall thickness. Finally, the stack is again heated to melt the wax and to separate individual test specimens which are then degreased, washed, dye-checked, and dried.

The specimens used in this study had the following dimensions:

Outside diameter:	2.200 ± 0.0002 inch
Inside diameter:	2.000 ± 0.0002 inch
Height:	0.450 ± 0.0002 inch

Specimens used for the determination of compressive strength had the same outside diameter and height but their wall thickness was only 0.075 inch. All machining was done with 320 grit metal-bonded diamond wheels. The surface finish of the specimens was 20 to 30 μinch AA* determined with a Clevite Brush Surfanalyser 150 System. The microstructure showed an average grain size of 20 to 30 μ, and the pycnometric density was 3.850 gm/cc. An emission spectrochemical analysis was made by the American Spectrographic Laboratories, Inc., San Francisco, Calif. The following amounts of oxides of the elements were detected:

Al	Principal constituent
Si	0.4 %
Mg	0.5 %
Ca	0.02 %
Na	--
Fe	0.12 %
Mn	0.001%
Ti	0.025%
Zr	0.005%
Ba	0.002%

2. Apparatus

The apparatus used in tensile measurements has been described in detail elsewhere[7] and has not been modified in this study. A block diagram of the apparatus and a photograph of the testing facility are shown in Figs. 1 and 2, respectively. The new part of the apparatus used in compressive work consists of a 9:1 pressure amplifier (Ruska, Model 2448), a 30,000 psi pressure transducer (B-L-H Type STD), the specimen holder and the pressurization sleeve, a precision 50,000 psi pressure gauge (Heise), an air driven pump having a 30,000 psi capacity (Sprague Engineering Model S-440-300), and the manifold connecting the pressure amplifier to the high pressure loop of the electrohydraulic system (MTS Division of Research, Inc., Minneapolis, Minn.).

*Arithmetical average as defined by the American Standards Association's ASA B46.1-1962 standard.

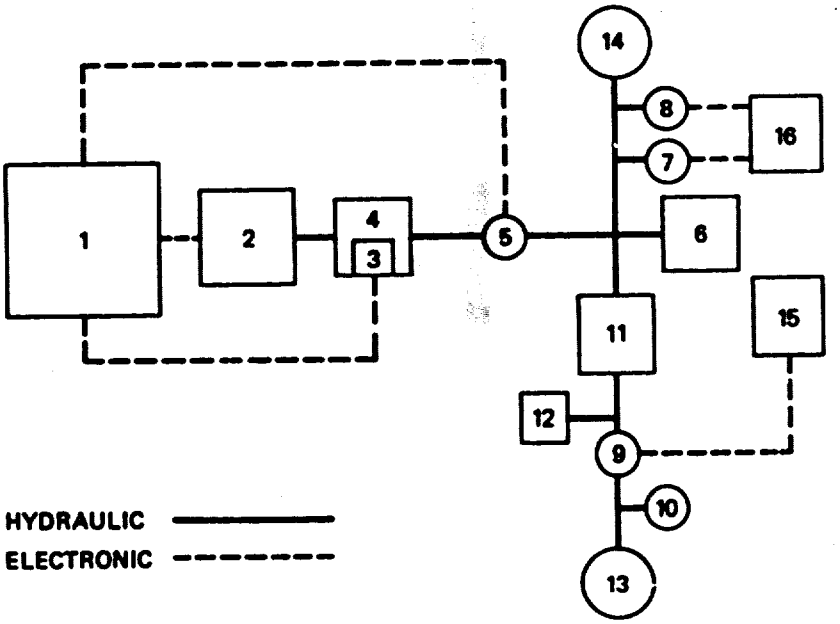

1 - CONTROL MODULE
2 - ELECTRIC PUMP
3 - SERVO VALVE
4 - HYDRAULIC RAM
5 - FEEDBACK TRANSDUCER
6 - DEAD WEIGHT GAUGE TESTER
7,8 - LOW PRESSURE MONITORING TRANSDUCERS
9 - HIGH PRESSURE MONITORING TRANSDUCERS
10 - 50,000 psi CALIBRATION GAUGE
11 - PRESSURE AMPLIFIER
12 - AIR DRIVEN 30,000 psi PUMP
13 - SPECIMEN HOLDER FOR COMPRESSIVE TESTING
14 - SPECIMEN HOLDER FOR TENSILE TESTING
15,16 - RECORDERS

TA-6012-25

FIG. 1 BLOCK DIAGRAM OF APPARATUS FOR MECHANICAL PROPERTIES TESTING

FIG. 2 MECHANICAL PROPERTIES TESTING FACILITY

The specimen holder and the compressive testing technique were originally developed at the Institute on an internally sponsored program.[8] The design of the specimen holder for compressive testing was controlled by the same principles on which the specimen holder for tensile testing is based. The test specimen is a thin-walled cylinder; hydrostatic pressure applied through a rubber sleeve to the outside wall of the specimen generates a tangential compressive stress in the specimen wall. Since the hydrostatic pressure is always normal to the surface on which it acts, and is uniform over the entire area of contact, no misalignment is possible and all parasitic stresses are eliminated, so long as the specimen geometry is nearly ideal. A unique feature of this test arrangement is that the end-faces of the specimen are under no compressive constraint and there is no friction between the specimen and the holder.

An exploded view of the specimen holder and the entire assembly for compressive testing are shown in Figs. 3 and 4. The specimen holder consists of the following parts: upper and lower confining block, spacer, a length of rubber tubing, and the pressurization sleeve. The upper confining block has a flange with six plain holes 60° apart on the same bolt circle for attaching the specimen holder to the pressurization sleeve. Below the flange, the body of the upper confining block is tapered on a 15° angle. The tapered section ends 5/8 inch below the flange in a flat shoulder approximately 0.050 inch wide. The section between the shoulder and the end-face is a straight cylinder and has a diameter of 2.200 ± 0.0005 inch, which is also the diameter of the lower confining block and of the outside of the test specimen. The end-face of the cylinder has a sharp, smooth outside edge and a flat-bottomed circular cavity whose center lies exactly in the axis of the cylinder. The bottom of the cavity and the outer edge of the end-face are parallel with each other and normal to the cylinder axis. The lower confining block is a cylinder whose bottom end-face has a rounded edge, while the upper end-face has a sharp outer edge and a cavity identical in shape, dimension, and location to the cavity in the upper confining block. The spacer is a cylinder whose diameter is 0.001 inch smaller than the diameter of the cavities of both confining blocks. The end-faces of the spacer are parallel

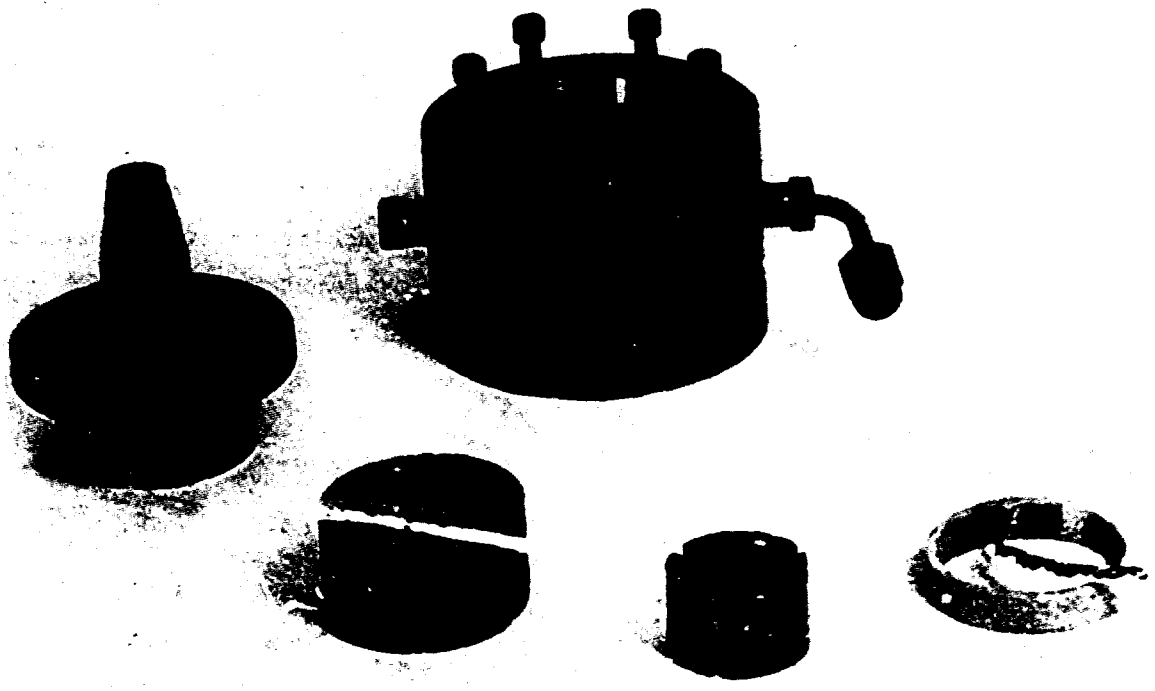

FIG. 3 EXPLODED VIEW OF SPECIMEN HOLDER FOR COMPRESSIVE TESTING

with each other and normal to the spacer's axis, along which a canal is drilled. Three slots, 120° apart, radiate from the canal to the outside of the spacer. These slots extend from one end-face through one-half the height of the spacer, and serve the purpose of admitting strain gauge lead wires into the canal of the upper confining block. The end-faces of both confining blocks containing the circular cavities face each other in the assembled specimen holder. They are flat only for a distance of approximately 0.005 inch from the edge inward. The rest of the end-faces slope on a 2° angle so that the gap between them widens toward the center. The reason for this is to accommodate the elongation of the test specimen due to Poisson's ratio.

The rubber tubing has a diameter somewhat smaller than the confining blocks over which it is stretched.

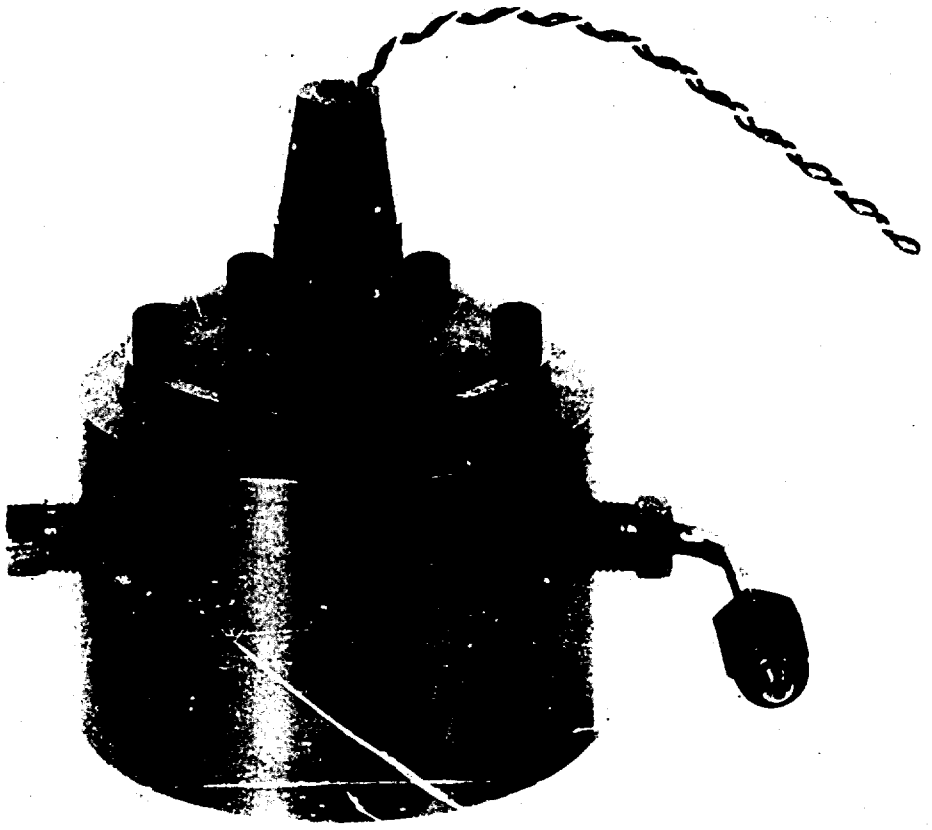

TA-6012-29

FIG. 4 ASSEMBLED SPECIMEN HOLDER FOR COMPRESSIVE TESTING

The pressurization sleeve is a thick walled cylinder whose inside diameter is 2.300 inch, except for the bottom 3/4 of an inch, where the inside diameter is 2.202 inch. Above this narrower section there is a groove holding a 2-1/4 inch x 2-3/8 inch x 1/16 inch O-ring. The upper inner edge of the sleeve is tapered on a 15° angle to position the tapered section of the upper confining block. Approximately in the middle of the sleeve are two holes opposite each other, one to admit the fluid, and the other to displace the air.

The specimen holder is assembled as follows:

The upper confining block is positioned with the end-face up; a 1-7/8 inch x 2 inch x 1/16 inch O-ring is forced over the straight section until it rests on the shoulder of the tapered section. The specimen is placed in position, resting on the end-face of the upper confining block.

When strain gauges are used, lead wires are threaded through the canal in the confining block. The spacer is placed with the slotted end down, such that the lead wires pass freely through the slots. The lower confining block is put in position resting on the spacer and making no contact with the specimen. The length of the spacer, therefore, is such that a gap of approximately 0.001 inch exists between the end-faces of the specimen and the confining blocks. A length of rubber tubing is slipped over the assembly covering the specimen and adjacent parts of both confining blocks. The tension of the rubber keeps the specimen aligned with the holder. The assembled holder is then forced into the pressurization sleeve; the tapered holes in the sleeve are matched with the holes in the flange of the upper confining block, and the assembly is bolted together. Finally, the air is bled out of the pressurization sleeve, the free space between the sleeve and the specimen in the holder is filled with water, and the entire assembly is clamped into a press and connected to the pressure manifold.

The strain measuring instrumentation consists of metal foil strain gauges, bridge supply and calibration units (Dynamics Instrumentation Co., Model 6179), dc amplifiers (Dynamics Instrumentation Co., Models 6460 and 6164), channel switching and balancing unit, and a Baldwin-Lima-Hamilton type "N" strain indicator. Three types of strain gauges were used, all manufactured by Micro-Measurement, Inc., Romulus, Michigan: Type MA-06-250AF-120 for axial strains (resistance, 120 $\pm$ 0.2 ohm; gauge factor, 2.08 $\pm$ 0.5%), type MA-06-250BF-120 for lateral strains (resistance, 120 $\pm$ 0.2 ohm; gauge factor, 2.05 $\pm$ 0.5%), and type MA-06-125TA-120, which are rosette gauges (resistance, 120 $\pm$ 0.2 ohm; gauge factor, 2.06 $\pm$ 1%). The strain gauges were attached to the thoroughly cleaned test specimens with BR-610 cement (W. T. Bean, Inc., Detroit, Michigan) using a procedure recommended by the manufacturer. The strain gauges were operated in the "half bridge" mode using dummy specimens with compensating gauges. The signals of the strain gauges and of the pressure transducers are recorded simultaneously on an oscillograph, or pressures and strains are determined in a step-wise fashion using the dead weight gauge tester or the Heise pressure gauge and reading the strain off the B-L-H strain indicator.

An alternative method of strain measurement was considered for use on this program, but proved unsuccessful. Since a detailed description is available in the literature,[9] only the main features of the method are presented here. The test specimen is the same ring as the one used in tensile and compressive work, and loading is accomplished by applying hydrostatic pressure. The strain in the specimen is sensed by a capacitance bridge in which the capacitor plates are mounted diametrically on the wall of the specimen. As the specimen is stressed, the spacing of the plates changes and the resulting change in capacitance is converted to a dc signal. This method works very well with small strains ($\varepsilon < 1 \times 10^{-6}$), for which the system can be calibrated against an interferometer, but it was not possible to obtain any reasonable calibration curve for the range of strains of interest in this work.

3. Procedure

a. Calibration

The calibration and operation procedure for tensile strength measurements has been described in detail previously[7] and has not been modified in the work described in this report.

In compressive testing, the 50,000 psi pressure gauge was used as a standard for calibrating the high pressure part of the system, because the maximum pressure obtainable with the dead weight gauge tester is only 10,000 psi, and in actual testing and calibration pressures up to 40,000 psi were used. The procedure is as follows: The valve (1) to the specimen holder is closed; the valve (2) in the line connecting the low pressure side of the pressure amplifier with the water reservoir is opened; the valve (3) between the air-driven pump and the high pressure side of the amplifier is opened; the pump is started, and the piston of the amplifier is driven back until it bottoms. Valves (2) and (3) are closed, and valve (4) to the pressure gauge and valve (5) connecting the MTS unit with the amplifier are opened; pressure is applied step-wise to the low end of the amplifier, and the resulting rise in the high pressure side is read off the gauge and displayed on the recorder. In this manner the system is checked for linearity over the entire pressure range used.

To make compressive strength measurements, the valve to the specimen holder is opened, the valve to the pressure gauge is closed. The air pump is used to pressurize the system to a few hundred psi, after which the valve to the air pump is closed. The MTS unit is programmed to generate the desired pressure level at a predetermined rate, and the test cycle is initiated.

For strain measurements, the same procedure is used in tension as in compression. The calibration is done by inserting into the circuit various precision resistors built into the power supplies which simulate the changes in the resistance of the strain gauge produced by dimensional changes. Because of the wide range of strains encountered, various combinations of power supplies and amplifiers had to be used.

b. Calculations

Maximum tensile stresses on the inner walls of test specimens were calculated using the formula

$$\sigma_{t\ max} = \frac{Pr_i^2}{r_o^2 - r_i^2} \left(1 + \frac{r_o^2}{r_i^2}\right)$$

where P is hydrostatic pressure at fracture (psi).

r_o is external radius (inches).

r_i is internal radius (inches).

The minimum tensile stresses on the outside walls of test specimens where tensile strain is measured were calculated by using the formula

$$\sigma_{t\ min} = \frac{2\ Pr_i^2}{r_o^2 - r_i^2}$$

The maximum compressive stresses on the inside walls of test specimens were calculated by using the formula

$$\sigma_{c\ max} = -\frac{2\ Pr_o^2}{r_o^2 - r_i^2}$$

Values of flexural strength were calculated by the formula

$$\sigma_f = \frac{M\,c}{I}$$

where M is bending moment (inch/lb).

c is distance from neutral axis to the outermost fibers (inch).

I is moment of inertia ($inch^4$).

The standard deviations (s.d.) were calculated from the formula

$$s.d. = \sqrt{\frac{\Sigma\, d^2}{n}}$$

where d is deviation from average strength value.

n is number of deviations.

Coefficients of variation are given by the formula

$$\frac{\text{standard deviation}}{\text{average ultimate strength}} \times 100$$

4. Strength Measurements

a. Compressive Strength

All compressive strength measurements were made at the stress rate of 10,000 psi/sec. The average ultimate compressive strength of Wesgo Al-995 alumina was found to be 448,000 ± 36,000 psi. Individual values are listed in Table A-I of Appendix A. The strength values found were higher than anticipated, so that hydrostatic pressures in excess of the equipment rating were required. Consequently, some minor equipment failures were encountered.

The high strength values indicate that the specimens did not fail in buckling. The critical buckling pressure for an externally pressurized, short, thin-walled tube is given by the formula[10,11]

$$P_c = \frac{E\,I}{r^3}(K^2 - 1)$$

where E is modulus of elasticity (psi).

I is moment of inertia ($inch^4$).

r is radius (inch).

K is a constant depending on the number of buckling nodes.

An unsupported ring under external pressure will tend to become elliptical and to buckle in the simplest mode with K = 2. In this case, the buckling pressure for rings used in this study would be 5250 psi. The test rings did not buckle under this pressure, and if buckling were the mode of fracture, K would have a value of nearly 5. It is therefore unlikely that the specimens failed in buckling.

Further proof of this contention is offered by the mode of fracture of the compressive specimens. It can be assumed that, if a specimen buckles, fracture occurs essentially in bending and results in a clean break in a line parallel to the specimen axis. This, however, was not the case. The failure of all compressive specimens occurred not in a line but over a zone approximately one-half inch wide which was larger on the inside of the specimen than on the outside in accordance with the stress distribution in the specimen wall. The material in the zone of the fracture was completely pulverized. A puzzling aspect of compressive failure is that all specimens showed extensive cracking in one or more lines parallel to the end-faces of the specimens. Whether this is the result of bending due to some end effects, or is the consequence of tensile strain due to Poisson's ratio is presently not known. It is not possible that it is the result of friction between the specimen and holder. To check this, the end-faces of the holder were inked prior to testing; no appreciable wear could be observed. A typical fracture line can be seen in Fig. 5, showing a specimen which was stressed to 452,000 psi (specimen No. 9 in Table A-I) and did not break (loading was interrupted at this level because of a failure of the equipment). The inside wall of the specimen also showed signs of extensive spalling which, unfortunately, are not visible in the picture.

b. Tensile Strength

The tensile strength of the test material was determined at three stress rates: at 100 psi/sec, the average ultimate tensile strength was 28,600 ± 700 psi (2.4%); at 1000 psi/sec, the strength was 31,000 ± 1000 psi (3.3%); and at 3000 psi/sec, the strength was 31,600 ± 1100 psi (3.6%). Individual strength data are presented in Table A-II of Appendix A.

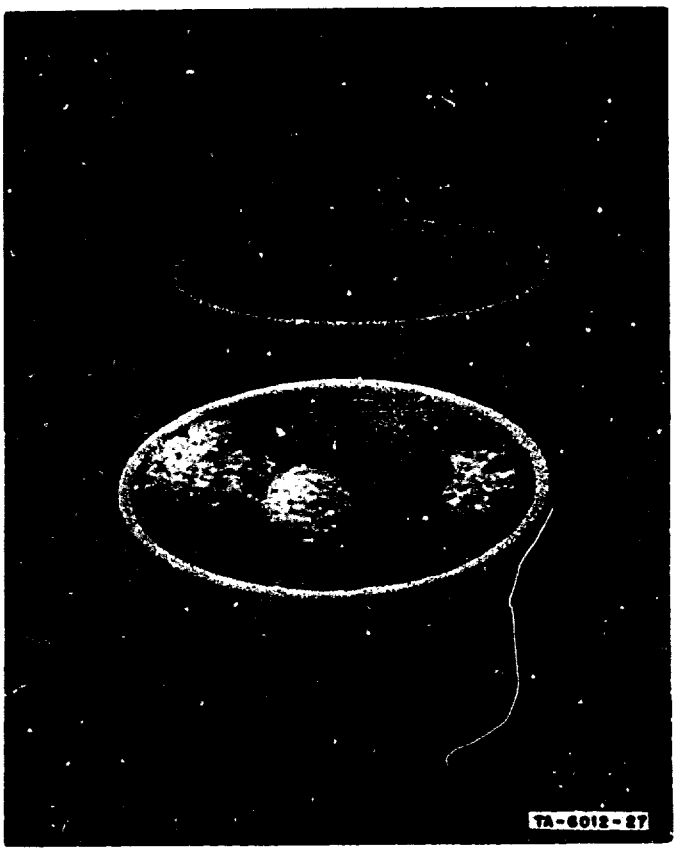

FIG. 5 SPECIMEN SHOWING INCIPIENT CRACK PARALLEL TO END-FACES

The relationship between stress rate and strength was not pursued further, because not enough specimens were available. The above data confirmed our previous findings that strength increases with increasing loading rate.[4] The strength data obtained in this study are somewhat higher than those determined previously, which may reflect the effect of a different grinding technique. Simultaneously with the above measurements, a series of identical experiments was made on a concurrent program (Contract N00019-67-C-0494) using Al-995 specimens from a lot ground by the manufacturer. These specimens were consistently weaker, e.g., their strength at the stress rate of 3000 psi/sec was 29,700 psi, which is the same as the value recorded previously for the same stress rate.[4]

c. Effect of Preloading on Ultimate Tensile Strength

A series of experiments was performed in which specimens were preloaded to certain fractions of their ultimate strength before their residual tensile strength was determined at the stress rate of 3000 psi/sec. The results of these tests are summed up in Table I and individual data are given in Tables VII and VIII of Appendix A.

Table I

EFFECT OF PRESTRESSING ON THE AVERAGE ULTIMATE TENSILE STRENGTH OF AL-995 ALUMINA ($\dot{\sigma}$ = 3000 psi/sec)

Prestressing	Magnitude (psi)	Number of Cycles	Ultimate Tensile Strength (psi)	Standard Deviation (± psi)	Coefficient of Variation (%)
None	0	0	31,600	1140	3.6
Compressive	336,000	0†	32,100	1320	4.1
Cyclic tensile	24,800/3500	10	32,800	1970	6.9
Cyclic tensile	24,800/3500	20	31,600	1800	5.7
Cyclic tensile	24,800/3500	40	32,300	1280	4.0
Cyclic tensile	24,800/3500	80	28,700	2510	8.7

†Samples were prestressed in a single stroke at the rate of 10,000 psi/sec

The effect of compressive preloading on the tensile strength was evaluated by stressing the specimens to 75% (336,000 psi) of their ultimate compressive strength at the stress rate of 10,000 psi/sec. No specimen broke under compressive stress. It can be seen in Table I that the residual tensile strength of these specimens was practically the same as the strength of specimens loaded directly to failure. Consequently, it can be assumed that a compressive stress of this magnitude applied under conditions used in this study does not alter the tensile strength of Al-995 alumina. It was also noticed that no cracks parallel with the end-faces developed.

A few shortcomings of the apparatus came to light during this study. It was noticed that after the application of the compressive load, all specimens were slightly wet. Consequently, all pieces of rubber used were checked for pinholes, but none were found. Also, changing the type of rubber used made no difference. It was therefore concluded that at high pressures rubber is permeable to water, and that another elastomer should be found. While the exposure to water apparently did not affect the test material in this study, it is conceivable that moisture could cause stress corrosion in long duration fatigue experiments. It was also found that in the present form the equipment is not very suitable for compressive cyclic fatigue testing, because of friction between the O-rings in the pressure amplifier. When a sinusoidal pressure function is programmed, the rising portion of the cycle is correct, but when the pressure decreases the piston does not retract evenly and reproducibly, and no two cycles are exactly alike.

The effect of cyclic tensile stresses on the ultimate tensile strength of Al-995 alumina was studied by exposing the specimens to a predetermined number of cycles between 3500 and 24,800 psi. The maximum stress corresponds to 80% of the ultimate tensile strength of this material determined at the stress rate of 3000 psi/sec. The stress ratio was 0.14 and the frequency was 4 cps. Individual groups of specimens were exposed to 10, 20, 40, and 80 cycles, respectively. No specimens of the first three groups failed in cyclic tension, but in the last group (80 cycles), three specimens broke after more than 50 cycles. The residual tensile strengths of all specimens are summarized in Table I. It can be seen that the effect on ultimate tensile strength of 10, 20, and 40 stress cycles is nil. However, there is a pronounced decrease in strength and increase in data scatter after exposure to 80 cycles, indicating that under these stress conditions some damage is incurred by the material; the results of the statistical analyses presented in Appendix B clearly show that the group of specimens subjected to 80 tensile cycles is significantly different (1% level) from all other groups. This fact agrees reasonably well with the results of the study of cyclic fatigue of alumina made under Contract No. AF 33(657)-10600.[7] The S-N curve for Al-995 alumina subjected to

cyclic stresses having a stress ratio of 0.14 indicates that for a maximum stress of 24,800 psi, the mean life N should be approximately 200 cycles. Considering the large data scatter commonly observed in fatigue testing, it is not surprising that three out of 15 specimens used in this series failed after less than 80 cycles.

d. Flexural Strength

The specimens used for flexural testing in this study were not part of the original lot of specimens used in the tensile and compressive work. Instead, they were obtained separately from R & W Products, Redwood City, California. Although they were machined from a green billet of Al-995 alumina and were fired at the Western Gold and Platinum Company, it is conceivable that a small difference in mechanical properties exists between the two lots of specimens. The specimens for the measurments of flexural strength were bars having a rectangular cross section and the following dimensions: length = 5.0 inch, width = 1.000 ± 0.001 inch, and thickness = 0.250 ± 0.0005 inch. The surface finish on the tensile side was 20 to 40 μinch AA.

Measurements of flexural strength were made at the Southern Research Institute, Birmingham, Alabama. All determinations were made in four-point loading at the stress rate of 3000 psi/sec. The inner and outer load points of the test fixture were provided with roller bearings to minimize friction and were spaced 2 and 4 inches apart, respectively. The average value of flexural strength obtained in this study was 36,900 ± 3000 psi (8.1%), which is in good agreement with other published data.[12] Individual values are compiled in Table IX of Appendix A.

5. Elastic Modulus and Poisson's Ratio

The results of this study show that the tensile and compressive elastic moduli of alumina are the same and that they are linear over the range of stresses employed. The average value of the elastic moduli was found to be $E = 53.6 \times 10^6 \pm 0.3 \times 10^6$ psi. These results are in excellent agreement with data obtained elsewhere in flexure on the same material.[13]

In the case of Poisson's ratio, the results are not so clear cut. In tension, the value of Poisson's ratio varies over the range of 0.20 to

0.22 and appears to be linear, within the experimental error, for each specimen tested. In compression, Poisson's ratio is higher and nonlinear, increasing with rising stress up to the value of 0.28 at the stress of 343,000 psi. Individual data points are compiled in Tables X and XI of Appendix A.

To our knowledge, this nonlinearity of Poisson's ratio in compression has never been observed except in the original work in which the compressive ring test technique was developed.[8] Although we cannot explain it, we are inclined to consider this nonlinearity to be real for several reasons. The value of Poisson's ratio can increase in two ways, i.e., by an actual increase of the lateral strain or by decrease of the principal strain. The former alternative is more logical, because for the latter an increase in μ would have to be accompanied by an increase in E. This was not observed. Furthermore, the same results were obtained both when the strains and the pressure were recorded continuously and simultaneously, and when strains and pressure were measured step-wise using the B-H-L strain indicator and the pressure gauge.

None of the stress-strain relationships studied on this program seem to contribute to an improved understanding of the theoretical correlation of flexural strength data with uniaxial tensile strength values. The fact that the tensile and compressive elastic moduli are the same eliminates the possibility of looking for a shift of the neutral axis which would normally occur in the direction of the higher elastic modulus value. As far as the nonlinearity of Poisson's ratio in compression is concerned, we do not presently know how to use it in considering the diversity of flexural and tensile strength data. Unsuccessful attempts to explain theoretically the dissimilarity of flexural and tensile strength have been made before, and some reasons for the failure of these attempts can be found in the literature.[14] There seems to be little point in using numerical conversion factors from the literature, because they are not based on any intrinsic material property and vary from one material to another. (In this program, the relationship of flexural strength to tensile strength can be described closely by the expression $\sigma_f = \sigma_t(1 + \mu)$, but the relationship is to be considered strictly fortuitous).

In conclusion, it has not been possible to attribute measured differences between uniaxial tensile strength and flexural strength values to any unusual elastic behavior of brittle materials. We have checked this difference by the most precise techniques available and have confirmed that it appears to be real, but the magnitude of the difference is considerably smaller than has been reported in the literature. It is still larger than can be accounted for by measurement errors in strength or elastic behavior, however, unless a real difference in properties can be attached to the two types of test specimens employed. In view of previously observed reproducibility of this material, the latter possibility seems unlikely. This problem will certainly not be resolved by means of the theory of elasticity. The answer will probably require a better understanding of the various fracture criteria and micromechanics of brittle materials.

SECTION IV

EFFECT OF IMPERFECT GEOMETRY ON THE MEASURED TENSILE STRENGTH OF INTERNALLY PRESSURIZED CYLINDRICAL TEST SPECIMENS

1. Background

The method of tensile testing of brittle materials[2] developed at Stanford Research Institute has produced strength data characterized by a very narrow scatter. The use of this method makes it possible to detect small changes of strength that are caused by some irregularity in the manufacturing process[3] or by changes in loading conditions.[4] The test specimen is a short thin-walled cylinder against whose inner surface hydrostatic pressure is applied through a rubber membrane, generating tangential tensile stresses in the specimen. Nearly uniaxial tensile loading can be achieved by the use of hydrostatic pressure, since this pressure is uniform over the entire area of contact and is normal to the confining surfaces. The assembled test fixture and specimen constitute a pressure vessel whose weakest part is the specimen itself, and hydrostatic pressure is the only force on the specimen. There are no compressive constraints exerted by the fixture, and there are no parasitic stresses from gripping the specimen. Only when the specimen is not perfectly round will stresses other than tangential tensile stresses be generated. Specimens made of oxide ceramics, carbides, etc., are diamond ground to final shape and dimensions. It is rather difficult not to make them round, but occasionally a specimen is found whose wall thickness varies by ± 0.0002 inch, usually in a completely random manner, and whose inside diameter may vary by as much as ± 0.0005 inch, indicating that the specimen is nearly elliptical. Specimen dimensions are measured with air gauges capable of discerning dimensional variations of a few one hundred thousandths of an inch. Departures from ideal roundness are caused by improper grinding techniques.

At this point it may be helpful to describe briefly the grinding procedure commonly used commercially in the preparation of large numbers of ring specimens on a production basis. The "as-fired" ring blanks are first faced so that they all have equal lengths and parallel faces. Then approximately 10 to 12 blanks are arranged in a stack. (Waxes or resins are used as mounting media.) The stacks are centerlessly ground to the final dimension of the outside diameter. Finally, the inside wall of the stack is finished on an internal cylindrical grinder. In this operation, the stack of specimens is put into a close-fitting collet. If the stack has to be forced into the collet, or if the collet transmits the gripping forces of a chuck or holding fixture, the stack will then deform slightly. After grinding, the inside of the stack is perfectly round while still in the collet. Once removed from the collet, however, the ceramic ring stack will return to its unstressed shape at the expense of true roundness. Fortunately, there are other grinding techniques such as that described in Section III that make it virtually impossible to make anything but round specimens.

2. Theoretical Study

The main purpose of this theoretical study was to provide an accurate method for calculating stresses in an internally pressurized cylinder of known ellipticity and to evaluate the error in stress calculations that was produced by treating the slightly elliptical ring as if it were a round one. The entire analysis is presented in Appendix C, and the results are summarized here.

Unlike the Mita-Timoshenko approach,[15,16] which assumes constant geometry of an elliptical ring under internal pressure, this analysis takes into account the fact that with increasing pressure the curvature of the elliptical ring, and therefore also the bending moment, change as the ring becomes more circular. In general, values of bending stresses calculated by this method are lower than those obtained by the classical method. It is found that for a given ring size (wall thickness) and degree of ellipticity, the maximum bending stresses increase with increasing value of Young's modulus of the test material. Conversely, bending stresses can be attenuated by increasing the wall thickness of the ring

made of a material having a high value of Young's modulus, or by decreasing the wall thickness in the case of materials having a low value of Young's modulus.

The maximum bending stresses are shown in Appendix C for alumina and graphite rings of identical geometry. For this case, the wall thickness is 0.1 inch, the nominal inside diameter is 2.000 inch, and the rings are 0.05% elliptical (b/a = 0.9995), which is the maximum out-of-roundness encountered in ceramic specimens machined by the procedure described above. For alumina at the nominal maximum tensile stress of 30,000 psi the value of the bending stress is 400 psi (1.3%) and for graphite at the nominal maximum tensile stress of 5000 psi, the bending stress is 42.3 psi (0.85%). These values are well within the 2 to 5% data scatter that is normally encountered in testing these materials.

3. Strength Measurements

To verify the results of the analytical study presented in Appendix C, actual strength measurements were performed using elliptical test specimens made of Plexiglas and ATJ graphite, and a photoelastic investigation was carried out using Columbia Resin CR-39 specimens.

The machining of elliptical specimens proved to be rather involved. First a computer program was established to produce the necessary tapes to operate a numerically controlled milling machine. Then, after programming, the machine produced templates (one for each degree of ellipticity), and from these templates, specimens were machined on a pantograph milling machine.

The inside perimeters of the machined rings were true ellipses and the wall thicknesses were constant in the sense that the distance between the inner and outer walls was the same along a line normal to the tangent at any point on the internal ellipse. Consequently, the outside perimeter of each ring was not truly elliptical. The short axis of all specimens was 2.000 ± 0.001 inches, and the wall thickness of each was 0.200 ± 0.001 inches. The height of the Plexiglas rings was 0.230 ± 0.001 inch. The Columbia Resin CR-39 specimens varied in height between 0.230 to 0.260 inch because of uneven thickness of the resin sheet from which they were made.

The first lot of Plexiglas specimens consisted of 60 pieces divided into six groups. The ellipticity of specimens of individual groups was varied in 1% increments from 0% to 5%. Initial strength measurements were made at a stress rate of 5000 psi/sec. Average strength values and standard deviations obtained are shown in Table II. Strength values for individual specimens are compiled in Table XVII in Appendix C.

TABLE II

AVERAGE ULTIMATE TENSILE STRENGTH OF
ROUND AND ELLIPTICAL PLEXIGLAS SPECIMENS
(Stress Rate, 5000 psi/sec)

Group	Ellipticity (%)	Average Ultimate Tensile Strength (psi)	Standard Deviation (± psi)	Coefficient of Variation (%)
A	0	15,380	420	2.7
B	1	15,730	690	4.4
C	2	15,840	400	2.5
D	3	15,730	660	4.2
E	4	15,860	310	2.0
F	5	15,320	570	3.7

The data in Table II clearly show that in the case of Plexiglas the effect of bending stresses due to ellipticity on the measured tangential tensile strength is nil. All 60 specimens can be treated as a single sample population having an average ultimate tensile strength of 15,640 ± 540 psi (3.4%), which is indistinguishable from any individual group.

From the theoretical analysis presented in Appendix C, it can be seen that, although the effect of ellipticity should be smaller than that usually calculated on the basis of the Mita-Timoshenko theory, the bending stresses in specimens of such a degree of out-of-roundness should be of considerable magnitude. Assuming the value of Young's modulus of Plexiglas to be $E = 0.45 \times 10^6$, the calculated values of bending stresses at failure (burst pressure of 2800 psi) should be approximately 500 psi for each 1% of ellipticity.

The exact reason for the observed uniformity of results is not known, but it appears reasonable to suspect that it is caused by the nonlinearity of Young's modulus of Plexiglas. It was found in the past that when this material is slowly loaded at a constant rate to high stress levels, it undergoes considerable plastic deformation. During plastic flow, the material yields to all applied stresses, including bending stresses which in the process become less severe, so that all specimens, regardless of the degree of out-of-roundness, show the same resistance to the applied force. Corroborating experimental evidence for this is found in the fact that the location of fracture often did not occur along the long axis of the specimen where maximum bending stress should exist. In some cases, when the fracture did not occur on either axis of the ellipse, the plane of fracture did not seem to be normal to the tangent at the point of failure, as if the specimen had a different configuration, such as that of a circular ring, at the moment of failure.

It is a known fact that for many materials such as plastics, the value of Young's modulus varies as a function of strain rate and stress level. It was shown in the case of Lucite,[17] which is closely related to Plexiglas, that the value of E can be changed from 0.42×10^6 to 0.95×10^6 psi by increasing the strain rate from 0.002 inch/inch/sec to 1.0 inch/inch/sec. This change is also accompanied by a considerable increase in the linearity of E.

It was considered that a similar relationship might exist in Plexiglas, in which case the effect of superimposed bending stresses should be more pronounced at higher stress rates (i.e., such that plastic flow no longer occurs). For this purpose, a new lot of specimens having 0%, 3%, and 5% ellipticity was machined from the original sheet of Plexiglas. Each group comprised five specimens which were tested at the stress rate of 50,000 psi/sec. Summary results are shown in Table III, and individual strength values are given in Table XVIII of Appendix C.

The data show that the ultimate tensile strength of Plexiglas increases with increasing stress rate (16,630 psi at 50,000 psi/sec versus 15,640 psi at 5000 psi/sec) and that the effect of ellipticity on the nominal tensile strength of this material is negligible even at the higher stress rate.

TABLE III

AVERAGE ULTIMATE TENSILE STRENGTH OF ROUND AND ELLIPTICAL PLEXIGLAS SPECIMENS (Stress Rate, 50,000 psi/sec)

Group	Ellipticity (%)	Average Ultimate Tensile Strength (psi)	Standard Deviation (± psi)	Coefficient of Variation (%)
A	0	16,510	690	4.2
D	3	16,780	200	1.2
F	5	16,610	330	2.2
A+D+F	0-5	16,630	590	3.6

However, there was a pronounced difference in the mode of fracture of these specimens. All elliptical specimens tested at the higher stress rate broke at or very near the major axis of the ellipse. In specimens tested previously at the stress rate of 5000 psi/sec, the location of failure was random. Furthermore, the elliptical specimens broken at 50,000 psi/sec show a multitude of fine planar cracks radiating from the inside wall in the vicinity of the major axis. In specimens having 5% ellipticity, these cracks seem to penetrate through approximately one-third of the wall thickness, whereas in specimens having 3% ellipticity, the layer of cracks is much shallower and is limited to a narrower region around the major axis. These cracks are shown in Fig. 6. No such cracks were found in the round specimens; therefore, it must be concluded that these cracks result from bending stresses caused by ellipticity. It should be noted that no cracks developed in identical elliptical specimens loaded at the stress rate of 5000 psi/sec. This means that a ten-fold increase in stress rate caused only enough stiffening in the test material to show the location and concentration of bending stresses but not enough to demonstrate the effect of bending stresses in terms of ultimate tensile strength. It is not known how high the stress rate must be to make Plexiglas behave in a truly brittle fashion. Furthermore, even if this factor should be established, it is doubtful that the results of such a study would be directly applicable to alumina.

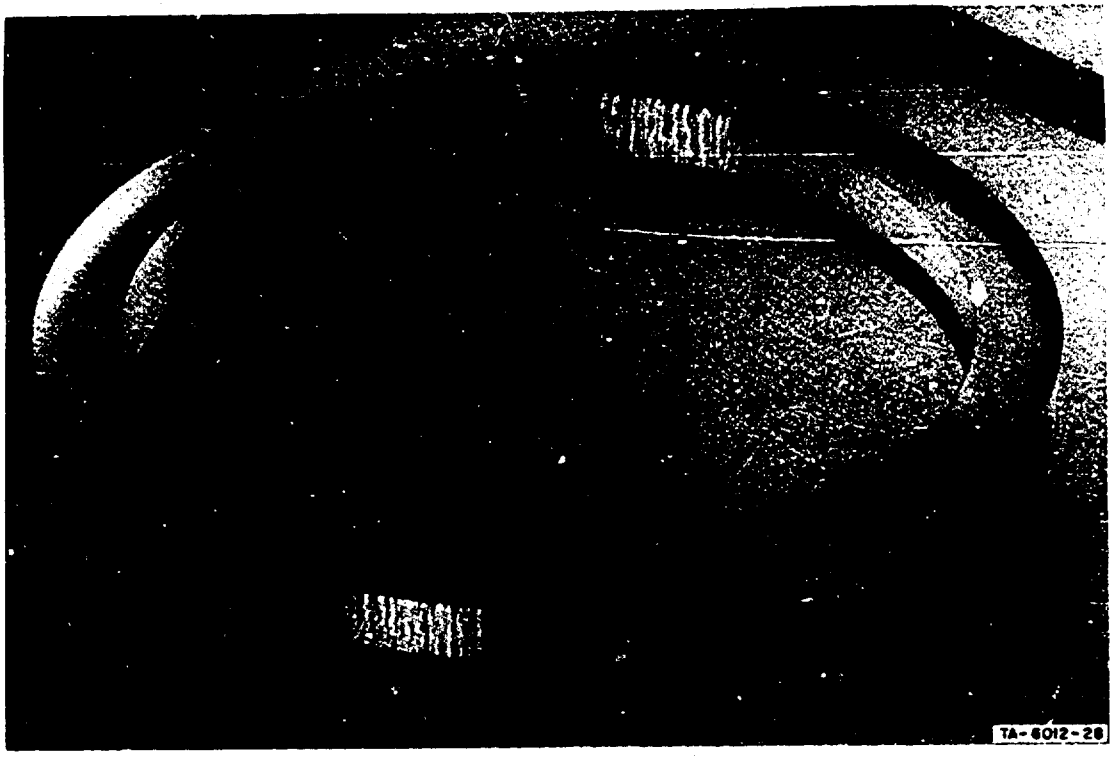

FIG. 6 CRACKS CAUSED BY BENDING STRESSES IN AN ELLIPTICAL PLEXIGLAS RING

Consequently, it was decided to use ATJ graphite for the determination of the effect of superimposed bending stresses, because this material could be expected to have a higher and more linear elastic modulus than Plexiglas at any presently obtainable loading rate. Three groups of specimens, with 0%, 3%, and 5% ellipticity, were machined. There were eight specimens in each group. Test specimens were milled from plates 3 inches x 3 inches x 0.250 inch which were cut from a large billet of graphite so that the grain orientation was the same in all plates. All specimens were tested at the stress rate of 50,000 psi/sec. Strength data are reported for only two groups of specimens (0% and 5% ellipticity), because an electronic failure of the pressure monitoring unit occurred during testing of specimens having intermediate ellipticity (3%). This breakdown was not detected until all specimens of this group were tested; the resulting pressure recordings were therefore completely meaningless.

Average ultimate tensile strength data and standard deviations for the remaining two groups of graphite specimens are shown in Table IV. Strength values for all specimens are presented in Table XVIII of Appendix C.

TABLE IV

AVERAGE ULTIMATE TENSILE STRENGTH OF ROUND AND ELLIPTICAL ATJ GRAPHITE SPECIMENS
(Stress Rate, 50,000 psi/sec)

Group	Ellipticity (%)	Average Ultimate Tensile Strength (psi)	Standard Deviation (± psi)	Coefficient of Variation (%)
A	0	4000	200	5.0
D	5	3020	140	4.5

These strength data are interesting in several respects. The average tensile strength of the round specimens (4000 psi) is much higher than the tensile strength (1790 psi) given for ATJ graphite in the Industrial Graphite Engineering Handbook. Actually, the strength value of 4000 psi is almost identical to the modulus-of-rupture value given in the handbook. Nevertheless, the tensile strength data for ATJ graphite obtained in this study are considered to be correct, since other workers[1] have obtained very similar strength values.

The average strength of specimens having 5% ellipticity is markedly lower (25%) than that of the round specimens, and this undoubtedly reflects the effect of superimposed bending stresses. On closer scrutiny, however, it is found again that the effect of bending stresses is considerably less than that predicted by theory. Taking the value of Young's modulus of ATJ graphite to be $E = 1.5 \times 10^6$ psi, the bending stresses at a bursting pressure of 720 psi will be approximately 2350 psi (Eq. 1, Section IV.4.b). If this bending stress is subtracted from the nominal maximum tensile stress of the perfectly round specimens, the 5% elliptical specimens should have had an average tensile strength of only 1650 psi, corresponding to a bursting pressure of 300 psi. This, obviously, is not the case.

We have concluded that, at the present time, our ability to demonstrate a quantitative correlation of experimental results with theoretical calculations is hampered by our limited knowledge of the exact nature of the relationship between Young's modulus and the stress rate and stress level of the test materials used. On the basis of this conclusion, further work along these lines was suspended. Pursuit of this activity seemed unwarranted because it was uncertain that the results of this study could be extrapolated to materials having a much higher elastic modulus, such as alumina.

4. Photoelastic Studies

a. Apparatus

In order to obtain fringe patterns corresponding to strain variations resulting from pressurizing out-of-round test specimens, a transparent specimen holder was designed and built. This holder works essentially the same as the holder used for strength measurements, but there are some differences in design. A schematic drawing of the transparent specimen holder is shown in Fig. 7. The holder consists of two rectangular plates of 1-inch-thick Plexiglas. In the center of each plate is a hole perpendicular to the face of the plate. On one side of the plate, the hole is undercut to accommodate a 1-5/16 inch x 1-1/8 inch x 3/32 inch "O" ring. On the same side of each plate, concentric with the hole is a circular groove about 1/8 inch deep and 1/8 inch wide. The outer diameter of the groove is 1.995 inches. The outside wall of the groove is normal to the face of the plate, but the inside wall is tapered on a 60° angle. In one of the plates there is a narrow canal for admission of the working fluid, which enters into the assembly in the space between the circular groove and the "O" ring.

The other components of the testing fixture are a perforated steel ring, a rubber diaphragm, a connecting shaft, two round cover plates, and washers. The perforated ring serves as a spacer which separates the two Plexiglas plates. The height of this ring is such that the distance between the plates in the assembled unit is 0.001 inch greater than the height of the test specimen positioned between the plates so

that no compressive constraint is exerted on the specimen. (Because individual specimens varied in height, due to the uneven thickness of the resin sheet from which they were machined, several such rings were made.) The perforated ring also serves as support for a thin rubber diaphragm which is stretched over its outer wall and positions the test specimen so that it is fully visible.

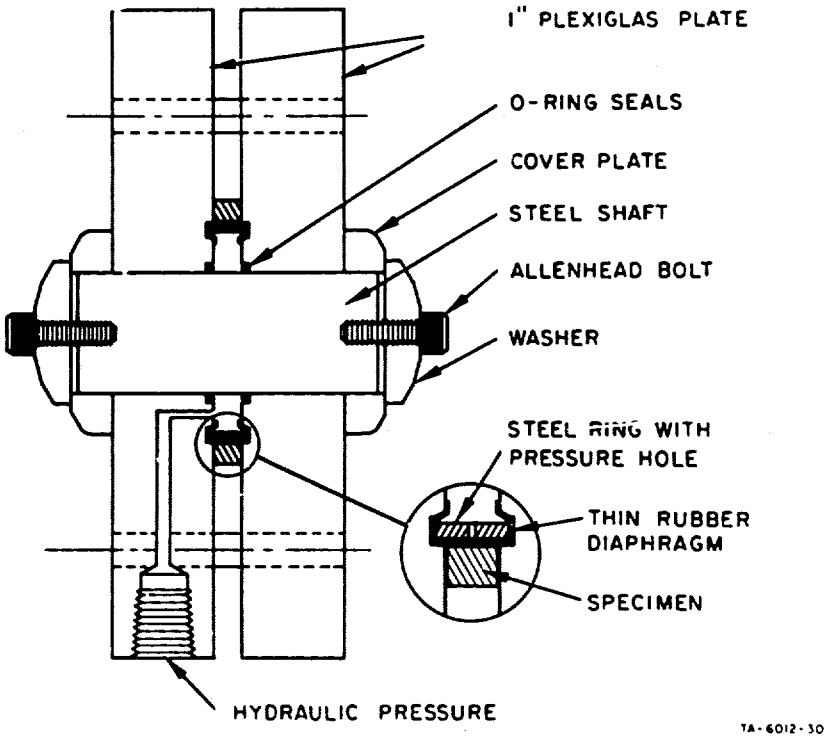

FIG. 7 SCHEMATIC DRAWING OF TRANSPARENT SPECIMEN HOLDER FOR PHOTOELASTIC STUDY

The unit is assembled as follows: the connecting shaft (diameter 1.125 inch) is pushed through the "O" ring in the plate containing the canal connected to the pressure line; a cover plate is slipped over the free end of the shaft and is secured by a washer and bolt arrangement; a short, thin-walled rubber tube is stretched over the perforated ring; the width of this tube is such that it overlaps the end-faces of the ring by about 3/16 inch, forming a free lip; the ring with the rubber

is forced into the groove in the Plexiglas plate; the lip of the rubber tube pushes against the inner wall of the groove, making a leakproof seal; a test specimen is placed around the ring and the second Plexiglas plate is pushed over the connecting shaft until the groove engages the free end of the perforated ring; finally, the second cover plate is placed in position and the entire assembly is tightened by turning the bolts in the ends of the connecting shaft. Hydrostatic pressure is generated by means of a dead weight gauge tester.

The optical train used in the photoelastic investigation consisted of a white light source, a condenser, a circular polarizer, the specimen in its holder, a circular analyzer, a green filter (Kodak Wratten No. 61), and a Princeton copy camera equipped with a 12-inch focal length lens. Because of creep problems at longer exposures and higher load levels, considerable time was spent in optimizing the combination of proper light conditions, length of exposure, lens opening, type of film, and development of film negatives before the final photographs were taken. The specimen holder and the optical train used in this study are shown in Fig. 8.

b. Experimental

In the analytical treatment of the stress distribution in the wall of an internally pressurized elliptical cylinder (Appendix C), a strictly elastic stress-strain relationship is postulated. The final expression derived for the maximum bending stress (S_b) whose locus is at the intercept of the major axis and the inner wall of the elliptical ring, is

$$S_b = \frac{3E\epsilon_o d}{4a}\left[1 - e^{-a^3 P/3EI}\right] \qquad (1)$$

in which E is Young's modulus, ϵ_o is initial ellipticity of the unpressurized ring, i.e., 1 - b/a, d is the specimen wall thickness, a is the average value of the major semiaxis, and I is the moment of inertia of the cross section per unit length. Values of S_b calculated in this manner were used together with the known radial and tangential stresses in a pressurized ring to predict the number of fringes, N, along the major

axis for various internal pressures and degrees of ellipticity using the equation

$$N = \frac{2(P + S_b)t}{f} \qquad (2)$$

where P is the internal pressure, S_b is the maximum bending stress, t is the height of the ring, and f is the fringe constant of the photoelastic material employed.

To calculate the number of fringes (using Eq. 2), it is necessary to know the value of Young's modulus and the fringe constant of the test material. These values were determined separately in flexure and were found to be $E = 0.265 \times 10^6$ psi and f = 95 psi per fringe. The predicted number of fringes and the actual fringe count are compared in Fig. 9. It can be seen that there is excellent agreement between experimental and theoretical data. Some representative fringe patterns obtained on specimens with various degrees of ellipticity are shown in Figs. 10 through 15. These pictures also corroborate the basic postulate of the theory presented--the fact that the geometry of out-of-round rings changes on pressurization. For instance, the original ellipticity of the ring shown in Fig. 15 was 5%. It can be readily ascertained--by measuring the two axes of the ring--that, at the internal pressure of 400 psi, the original ellipticity is reduced to approximately 1.0%.

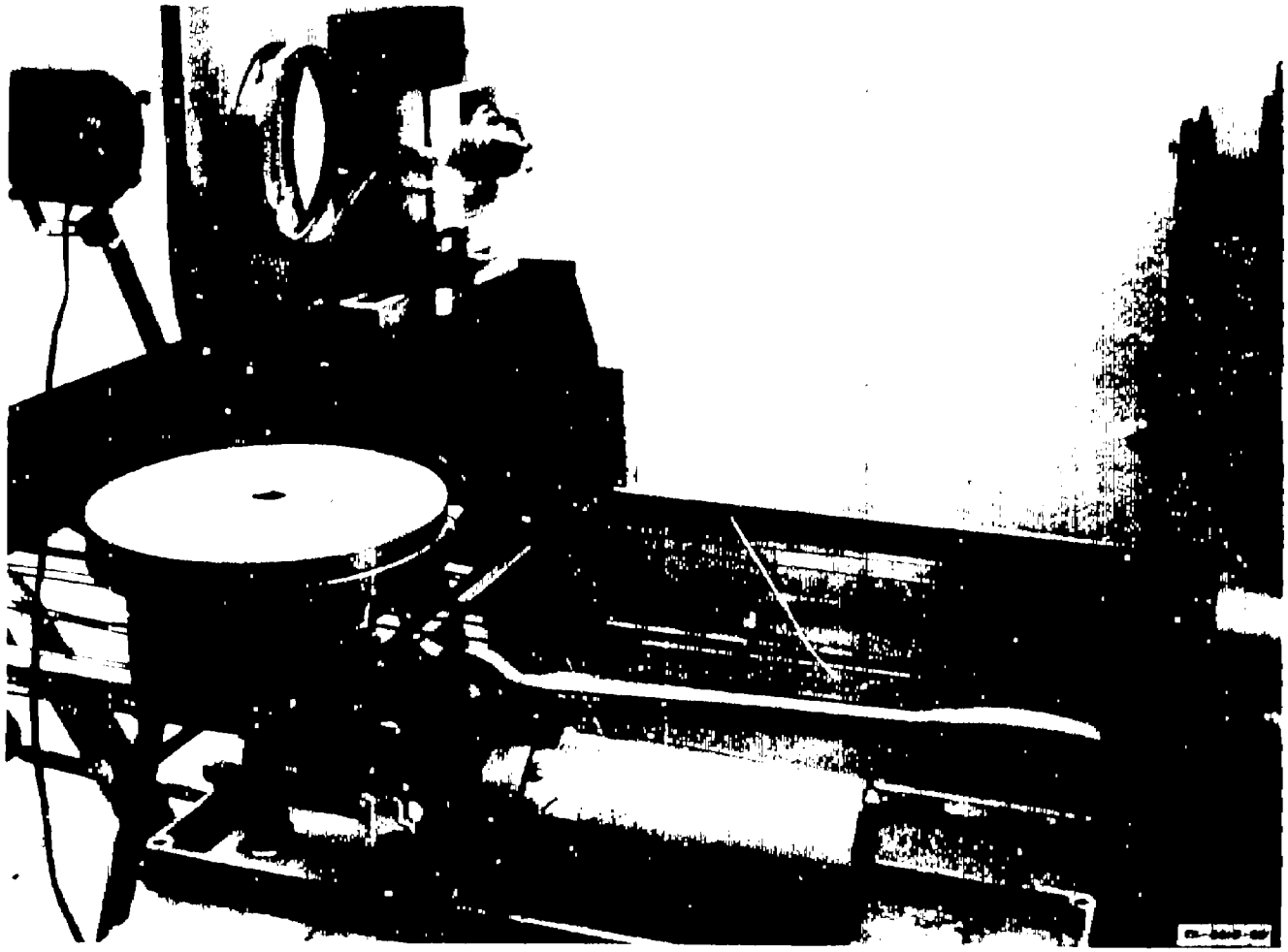

FIG 8 SPECIMEN HOLDER AND OPTICAL TRAIN FOR PHOTOELASTIC STUDY

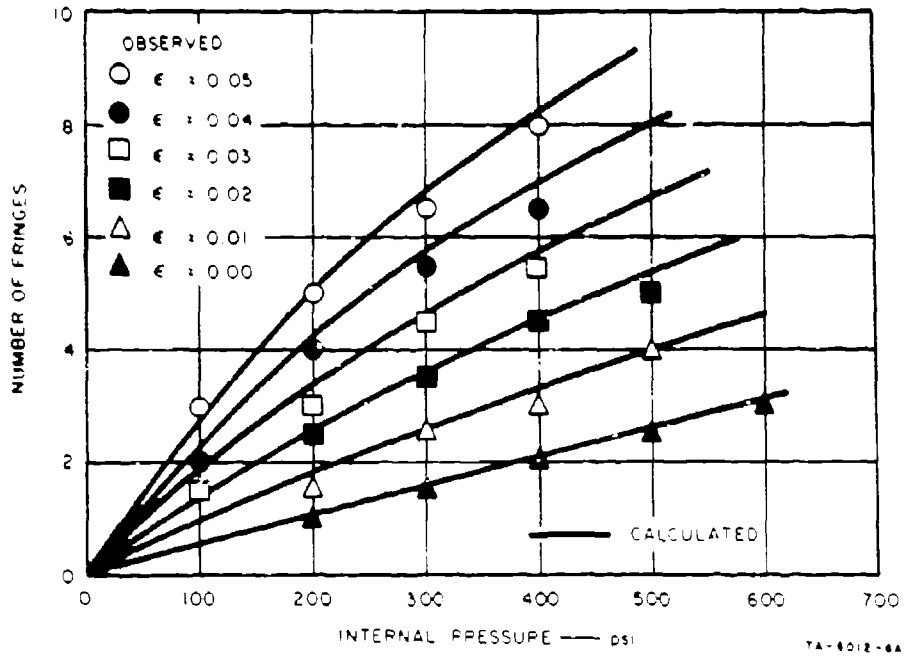

FIG. 9 COMPARISON OF PREDICTED AND EXPERIMENTALLY VERIFIED NUMBER OF FRINGES IN CR-39 SPECIMENS

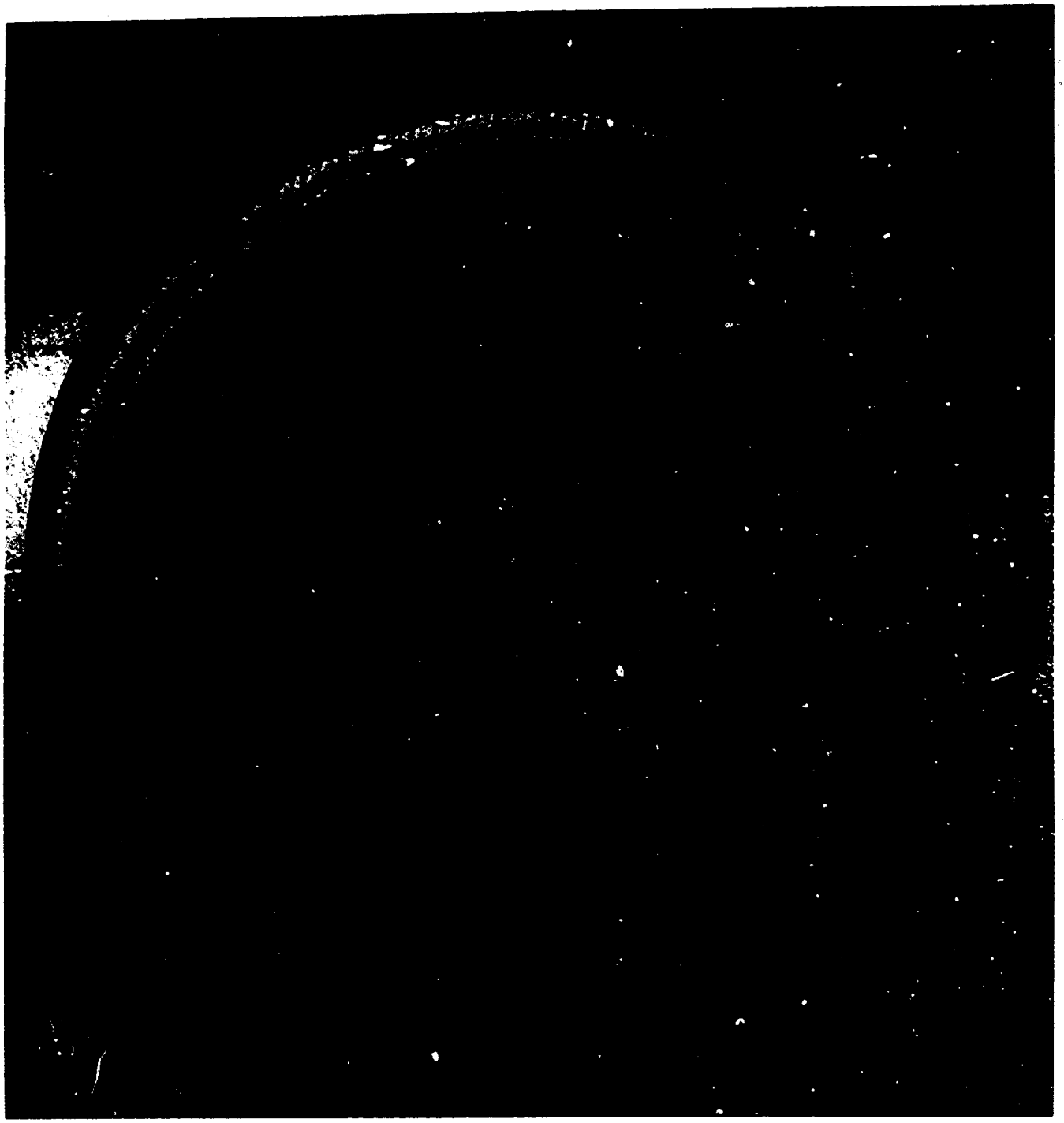

FIG. 10 FRINGE PATTERN IN A CR-39 TEST SPECIMEN WITH AN INITIAL ELLIPTICITY ϵ_0 - 0% UNDER 400 psi INTERNAL PRESSURE

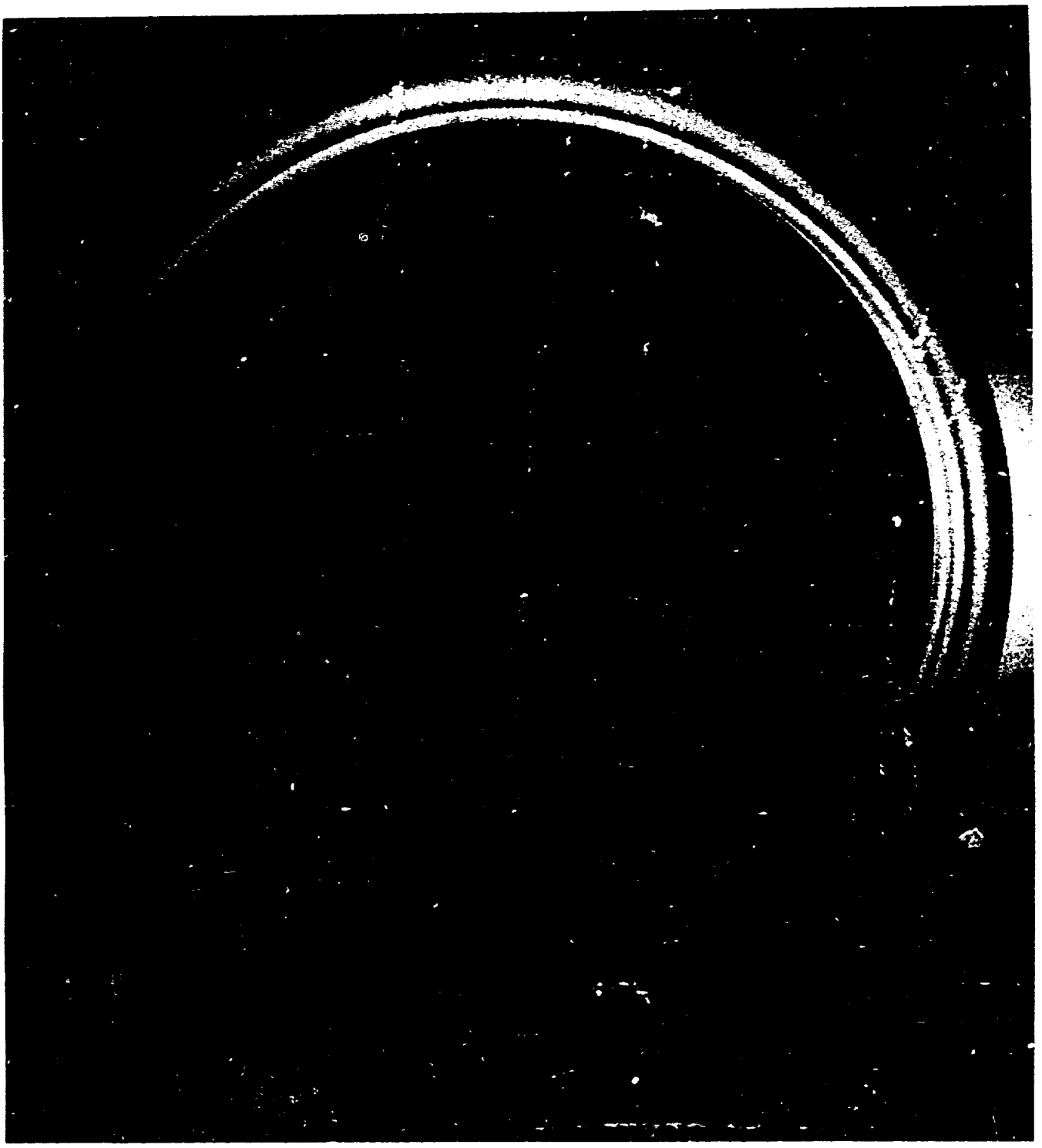

FIG. 11 FRINGE PATTERN IN A CR-39 TEST SPECIMEN WITH AN INITIAL ELLIPTICITY ϵ_0 = 1% UNDER 400 psi INTERNAL PRESSURE

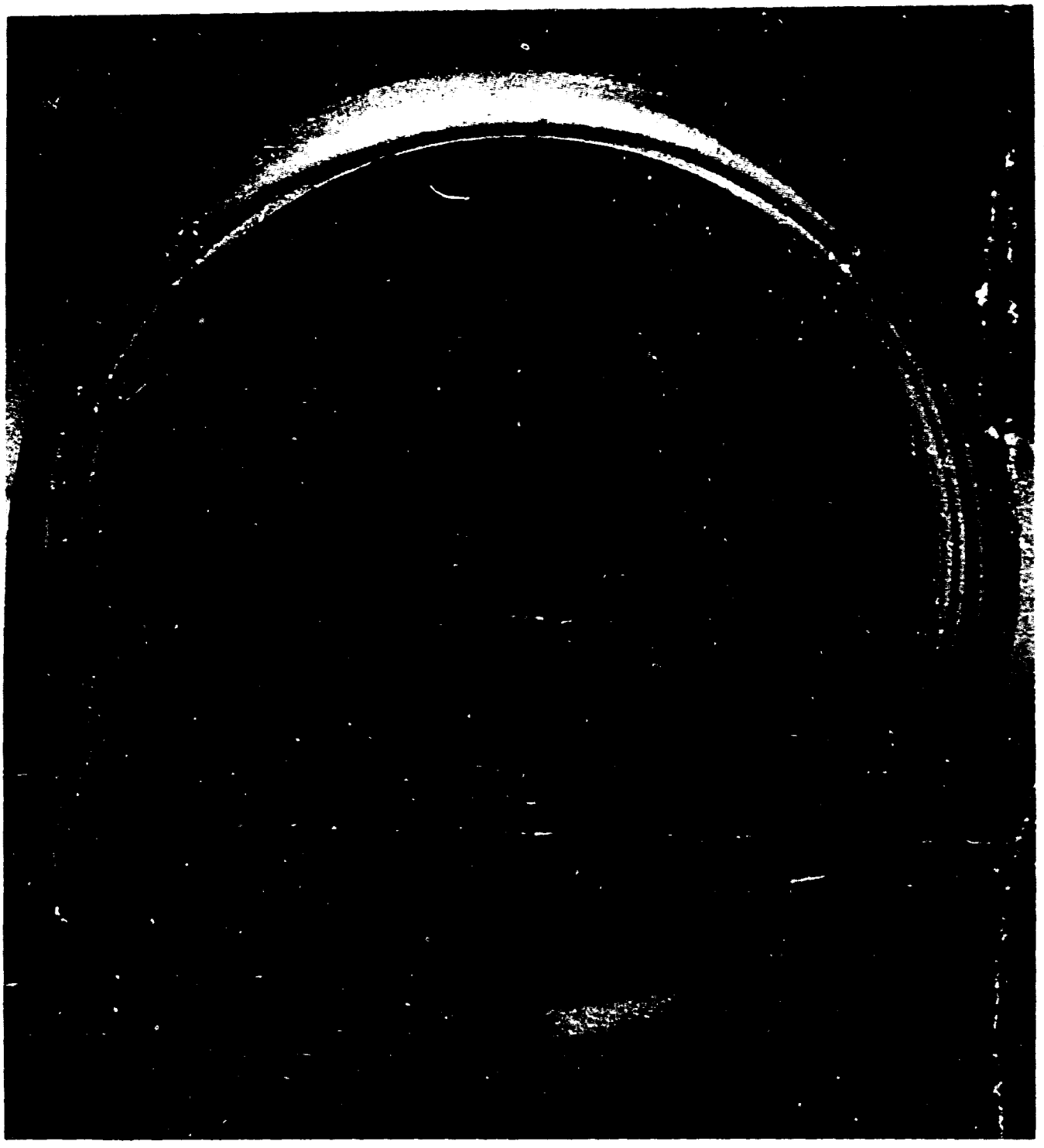

FIG. 12 FRINGE PATTERN IN A CR-39 TEST SPECIMEN WITH AN INITIAL ELLIPTICITY ϵ_0 = 2% UNDER 400 psi INTERNAL PRESSURE

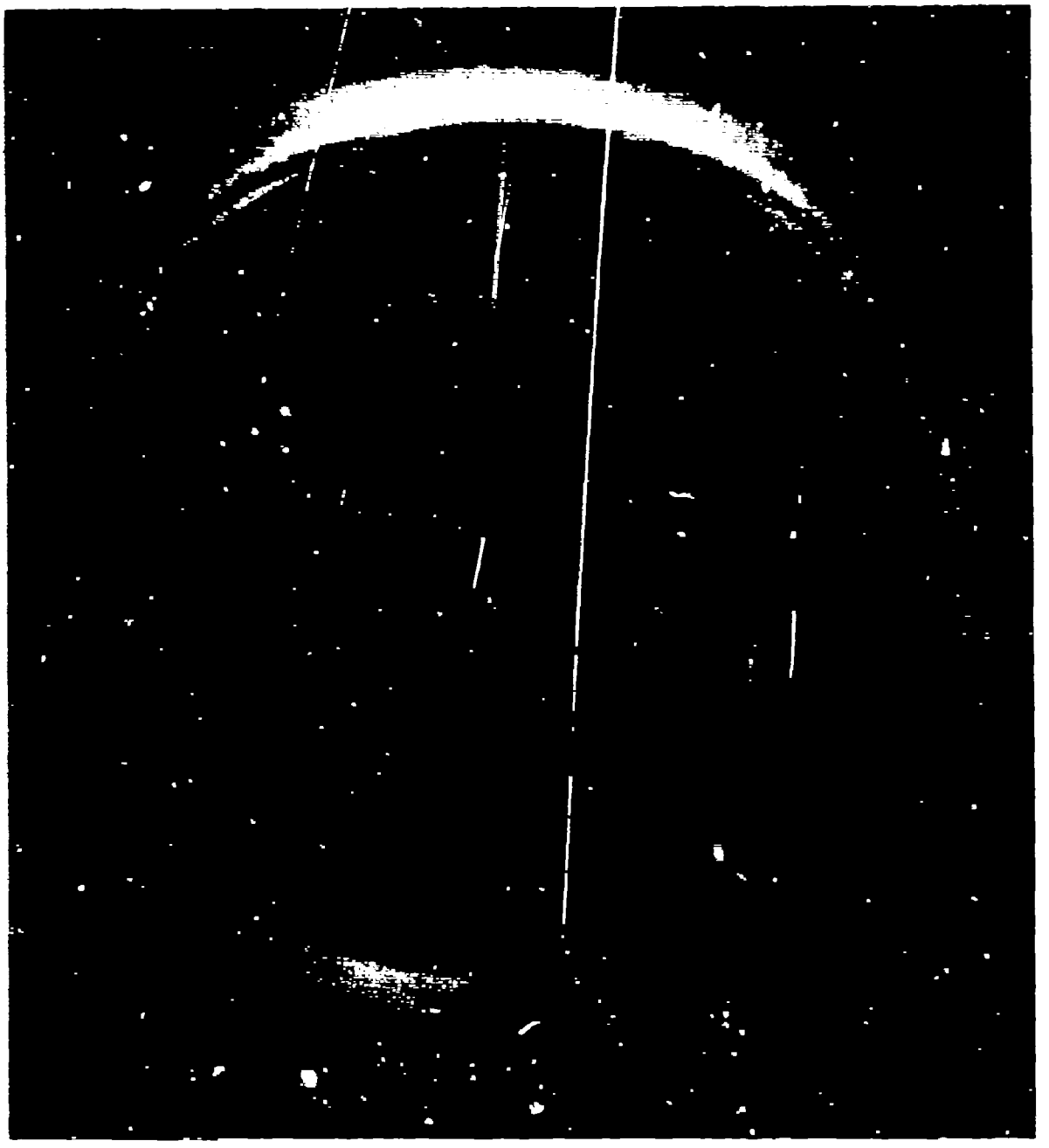

FIG 13 FRINGE PATTERN IN A CR-39 TEST SPECIMEN WITH AN INITIAL ELLIPTICITY [illegible] = 3% UNDER 400 psi INTERNAL PRESSURE

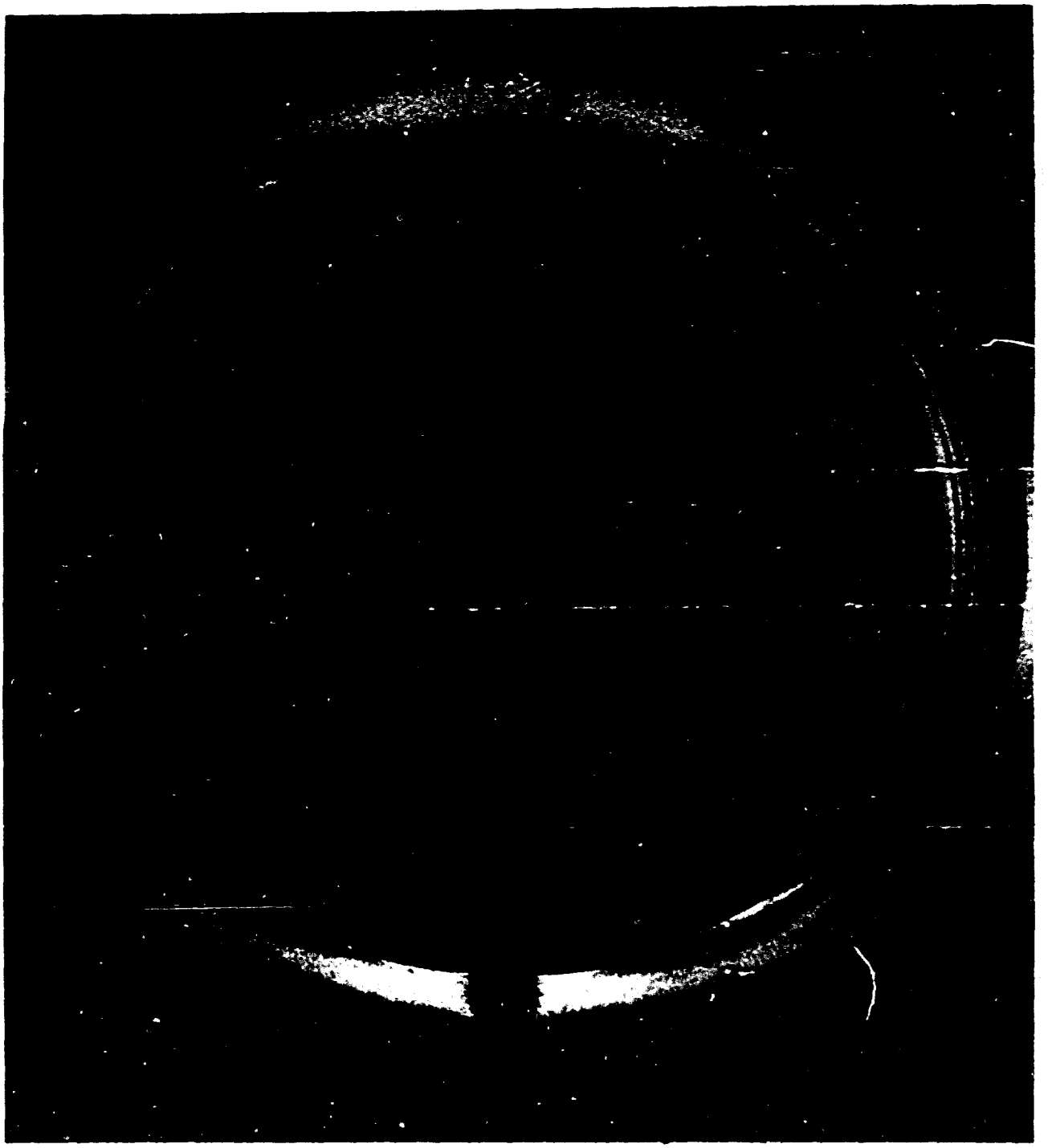

FIG. 14 FRINGE PATTERN IN A CR-39 TEST SPECIMEN WITH AN INITIAL ELLIPTICITY ϵ_0 = 4% UNDER 400 psi INTERNAL PRESSURE

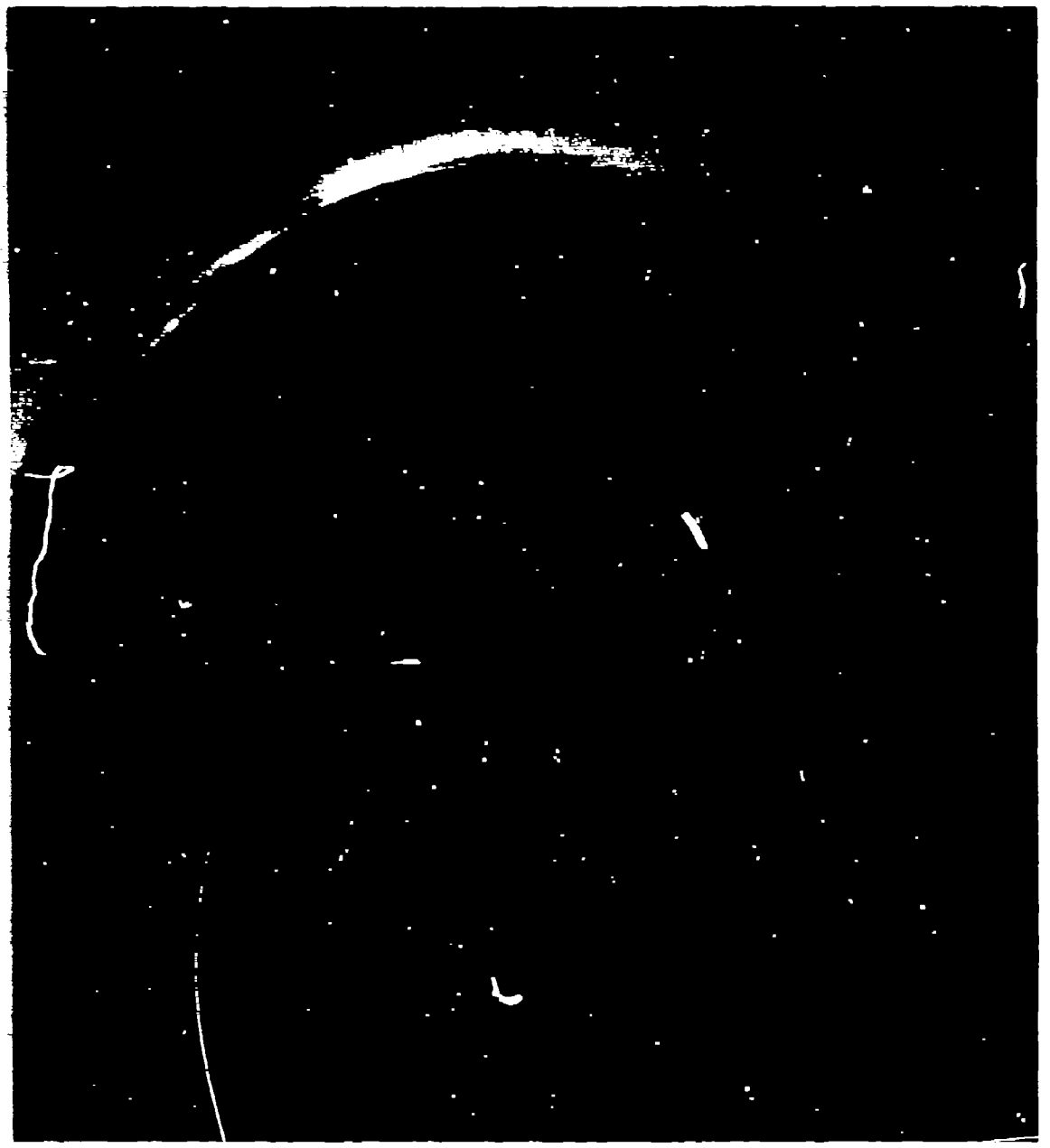

FIG. 15 FRINGE PATTERN IN A CR-39 TEST SPECIMEN WITH AN INITIAL ELLIPTICITY [illegible] UNDER 400 psi INTERNAL PRESSURE

APPENDIX A

EXPERIMENTAL DATA OBTAINED ON AL-995 ALUMINA

TABLE V

COMPRESSIVE STRENGTH OF AL-995 ALUMINA

Specimen Number	Stress Rate (psi/sec)	Ultimate Compressive Strength (psi)	Deviation (psi)
1	10,000	439,000	- 9,000
2	10,000	428,000	- 20,000
3	10,000	460,000	+ 12,000
4	10,000	431,000	- 17,000
5	10,000	462,000	+ 14,000
6	10,000	414,000	- 34,000
7	10,000	447,000	- 1,000
8	10,000	406,000	- 42,000
9	10,000	452,000	+ 4,000
10	10,000	551,000	+103,000
11	10,000	455,000	+ 7,000
12	10,000	425,000	- 23,000

Average Ultimate Compressive Strength: 448,000 psi

Standard Deviation: ± 36,000 psi

Coefficient of Variation: 8.0%

Preceding Page Blank

TABLE VI

ULTIMATE TENSILE STRENGTH OF AL-995 ALUMINA

Specimen Number	Stress Rate (psi/sec)	Ultimate Tensile Strength (psi)	Deviation (psi)
1	100	28,400	- 300
2	100	28,400	- 300
3	100	29,800	+ 1100
4	100	28,000	- 700
Average	100	28,700	± 690 (2.4%)
1	1000	32,200	+ 1200
2	1000	30,700	- 300
3	1000	29,500	- 1500
4	1000	31,600	+ 600
Average	1000	31,000	±1100 (3.5%)
1	3000	30,600	- 1000
2	3000	30,700	- 900
3	3000	31,600	0
4	3000	32,100	+ 500
5	3000	30,100	- 1500
6	3000	30,700	- 900
7	3000	32,700	+ 1100
8	3000	31,100	- 500
9	3000	33,800	+ 2200
10	3000	30,400	- 1200
11	3000	32,800	+ 1200
12	3000	32,800	+ 1200
Average	3000	31,600	±1100 (3.5%)

TABLE VII

ULTIMATE TENSILE STRENGTH OF AL-995 ALUMINA AFTER EXPOSURE TO A COMPRESSIVE STRESS OF 336,000 PSI

Specimen Number	Stress Rate (psi/sec)	Ultimate Tensile Strength (psi)	Deviation (psi)
1	10,000	31,600	- 500
2	10,000	32,400	+ 300
3	10,000	31,300	- 800
4	10,000	29,400	- 2700
5	10,000	33,100	+ 1000
6	10,000	34,000	+ 1900
7	10,000	32,400	+ 300
8	10,000	32,300	+ 200
9	10,000	33,500	+ 1400
10	10,000	32,700	+ 600
11	10,000	29,800	- 2300
12	10,000	32,700	+ 600

Average Ultimate Tensile Strength: 32,100 psi

Standard Deviation: ± 1,320 psi

Coefficient of Variation: 4.1%

TABLE VIII

ULTIMATE TENSILE STRENGTH OF AL-995 ALUMINA
AFTER EXPOSURE TO CYCLIC TENSILE STRESSES
(Maximum Stress, σ_{max} = 24,800 psi; Stress Ratio R = 0.14)

Specimen Number	Stress Rate (psi/sec)	Number of Cycles	Ultimate Tensile Strength (psi)	Deviation (psi)
1	3000	10	33,400	+ 600
2	3000	10	31,200	- 1600
3	3000	10	31,400	- 1400
4	3000	10	33,000	+ 200
5	3000	10	33,600	+ 800
6	3000	10	34,400	+ 1600
7	3000	10	32,000	- 800
8	3000	10	35,100	+ 2300
9	3000	10	33,100	+ 300
10	3000	10	34,900	+ 2100
11	3000	10	33,800	+ 1000
12	3000	10	27,600	- 5200
Average	3000	10	32,800	± 2000 (6.0%)
1	3000	20	32,900	+ 1300
2	3000	20	29,500	- 2100
3	3000	20	32,400	+ 800
4	3000	20	30,200	- 1400
5	3000	20	29,500	- 2100
6	3000	20	28,000	- 3600
7	3000	20	31,700	+ 100
8	3000	20	32,000	+ 400
9	3000	20	34,600	+ 3000
10	3000	20	32,400	+ 800
11	3000	20	32,900	+ 1300
12	3000	20	32,800	+ 1200
Average	3000	20	31,600	± 1800 (5.7%)

TABLE VIII(Concluded)

ULTIMATE TENSILE STRENGTH OF AL-995 ALUMINA
AFTER EXPOSURE TO CYCLIC TENSILE STRESSES
(Maximum Stress, σ_{max} = 24,800 psi; Stress Ratio R = 0.14)

Specimen Number	Stress Rate (psi/sec)	Number of Cycles	Ultimate Tensile Strength (psi)	Deviation (psi)
1	3000	40	32,100	- 200
2	3000	40	33,800	+ 1500
3	3000	40	32,000	- 300
4	3000	40	33,100	+ 800
5	3000	40	30,600	- 1700
6	3000	40	29,100	- 3200
7	3000	40	32,300	0
8	3000	40	32,000	- 300
9	3000	40	32,800	+ 500
10	3000	40	33,200	+ 900
11	3000	40	33,800	+ 1500
12	3000	40	32,800	+ 500
Average	3000	40	32,300	± 1300 (4.0%)
1	3000	80	31,600	+ 2900
2	3000	80	33,100	+ 4400
3	3000	80	30,200	+ 1500
4	3000	80	28,700	0
5	3000	80	28,500	- 200
6	3000	80	25,800	- 2900
7	3000	80	25,900	- 2800
8	3000	76	FAILED	
9	3000	80	25,400	- 3300
10	3000	80	27,600	- 1100
11	3000	54	FAILED	
12	3000	80	28,000	- 700
13	3000	75	FAILED	
14	3000	80	32,400	+ 3700
15	3000	80	26,900	- 1800
Average	3000	80	28,700	± 2500 (8.7%)

TABLE IX

FLEXURAL STRENGTH OF AL-995 ALUMINA

Specimen Number	Stress Rate (psi/sec)	Ultimate Flexural Strength (psi)	Deviation (psi)
1	3000	30,240	- 6700
2	3000	31,250	- 5600
3	3000	38,210	+ 1300
4	3000	38,300	+ 1400
5	3000	36,480	- 400
6	3000	38,690	+ 1800
7	3000	37,580	+ 700
8	3000	38,400	+ 1500
9	3000	38,880	+ 2000
10	3000	37,580	+ 700
11	3000	Broken Accidentally	
12	3000	39,890	+ 3000

Average Ultimate Flexural Strength: 36,900 psi

Standard Deviation: ± 3,000 psi

Coefficient of Variation: 8.1%

TABLE X

ELASTIC MODULUS AND POISSON'S RATIO OF AL-995 ALUMINA IN TENSION

E = Elastic modulus (psi x 10^6)
σ = Stress (psi)
μ = Poisson's ratio
ϵ_1 = Axial strain (μin./in.)
ϵ_2 = Lateral strain (μin./in.)

Specimen No. 1					Specimen No. 3		
σ	ϵ_1	E	ϵ_2	μ	σ	ϵ_1	E
3,520	68	53.3	13	0.200	4,400	84	52.4
5,760	108	53.2	23	0.212	8,800	165	53.3
8,420	157	53.6	36	0.214	10,120	190	53.3
10,080	188	53.7	39	0.210	13,560	255	53.2
13,250	246	53.8	51	0.209	14,450	269	53.7
16,780	314	53.5	64	0.205	19,950	371	53.8
19,430	361	53.8	73	0.203	22,370	417	53.6
22,400	418	53.6	85	0.204	28,020	520	53.9
26,370	494	53.4	103	0.209			
27,690	518	53.5	107	0.207			
Specimen No. 2					Specimen No. 4		
5,000	93	53.8	20	0.215	5,000	95	52.5
9,760	181	53.9	38	0.210	9,240	175	52.8
14,520	271	53.6	54	0.199	14,290	268	53.3
19,290	360	53.6	72	0.200	16,190	303	53.4
20,240	379	53.4	75	0.198	17,680	330	53.6
22,140	412	53.7	84	0.204	22,380	420	53.3
24,050	449	53.6	93	0.207			

TABLE X (Concluded)

ELASTIC MODULUS AND POISSON'S RATIO OF AL-995 ALUMINA IN TENSION

E = Elastic modulus (psi x 10^6)
σ = Stress (psi)
μ = Poisson's ratio
ε_1 = Axial strain (μin./in.)
ε_2 = Lateral strain (μin./in.)

Specimen No. 5					Specimen No. 6		
σ	ε_1	E	ε_2	μ	σ	ε_1	E
3,730	69	54.1	15	0.220	4,950	91	54.2
8,050	112	54.0	24	0.218	12,570	235	53.5
8,500	158	53.8	35	0.220	20,160	376	53.6
10,900	202	54.0	45	0.222	28,170	524	53.8
14,200	263	54.0	58	0.220	Specimen No. 7		
16,450	305	53.9	67	0.219			
19,750	363	54.4	79	0.217	4,690	88	53.3
22,110	409	54.2	91	0.223	10,350	194	53.4
27,040	498	54.3	111	0.223	15,180	282	53.8
					20,700	388	53.4
					27,330	512	53.4

TABLE XI

ELASTIC MODULUS AND POISSON'S RATIO OF AL-995 ALUMINA IN COMPRESSION

E = Elastic modulus (psi x 10^6)
σ = Stress (psi)
μ = Poisson's ratio
ε_1 = Axial strain (μin./in.)
ε_2 = Lateral strain (μin./in.)

Specimen No. 1					Specimen No. 4		
σ	ε_1	E	ε_2	μ	σ	ε_1	E
81,700	1520	53.8	362	0.238	62,950	1180	53.4
145,200	2740	53.0	620	0.226	128,390	2410	53.3
209,730	3920	53.5	1025	0.261	181,620	3400	53.4
269,700	5050	53.4	1350	0.267	261,160	4870	53.6
316,900	5980	53.0	1645	0.275	278,700	5240	53.2
345,700	6540	52.9	1720	0.263	343,200	6400	53.6
Specimen No. 2					Specimen No. 5		
69,170	1320	52.4	327	0.247	57,620	1060	54.5
131,120	2440	53.7	636	0.260	116,390	2160	53.8
193,670	3600	53.8	966	0.268	175,740	3290	53.4
255,620	4710	54.3	1314	0.279	259,290	4800	53.8
306,740	5620	54.6	1590	0.283	314,020	5860	53.6
342,820	6280	54.6	1780	0.283	357,240	6630	53.9
Specimen No. 3							
32,270	600	53.8	144	0.240			
118,120	2190	53.9	550	0.251			
172,860	3240	53.4	830	0.255			
202,820	3790	53.5	980	0.258			
230,480	4280	53.7	1110	0.258			
258,130	4790	53.9	1250	0.261			
288,670	5330	54.2	1390	0.261			
316,440	5820	54.4	1530	0.263			
345,710	6350	54.4	1660	0.262			

APPENDIX B

STATISTICAL ANALYSIS OF THE EFFECT OF PRESTRESSING ON ULTIMATE TENSILE STRENGTH

Preceding Page Blank

The objective of this work was to establish by means of statistical analysis of test data whether the ultimate tensile strength of ceramics is affected by prestressing. The data for this analysis are taken from Tables VI , VII , and VIII. The following tests were made:

(1) Analysis of variance to test the null hypothesis that the means of the populations from which the six samples were drawn are all equal (see Table XII).

(2) Analysis of variance to test the above hypothesis on the first five samples, omitting the set subjected to 80 tensile cycles (see Table XIII).

(3) T-test in which pairs of samples are compared under the assumption that each came from a population having equal variances. The null hypothesis in this case is that the means are equal (see Table XIV).

(4) The nonparametric U-test in which no assumption is made as to the type of parent populations from which each sample was drawn. This test compares two samples by rank-ordering the pooled sample and using the sums of the ranks in either sample as the test statistic (Z) (see Table XV).

Preceding Page Blank

TABLE XII

ANALYSIS OF VARIANCE
(All sets)

Source	Sum of Squares of Ultimate Tensile Strengths*	Degrees of Freedom	Mean Square	Computed F	Table Value of F
Between Groups	11,803	5	2,361	6.9	3.33
Within Groups	22,815	67	341		
Total	34,618	72			

*Values have been truncated.

Result: $F_{.01,5,67} = 3.33 < 6.9$; the computed F value exceeds the table value of F at the 1% level, indicating a highly significant difference between the means of the sets compared. Null hypothesis must be rejected.

TABLE XIII

ANALYSIS OF VARIANCE
(All sets except 80-cycle set)

Source	Sum of Squares of Ultimate Tensile Strengths*	Degrees of Freedom	Mean Square	Computed F	Table Value of F
Between Groups	1,229	4	307	1.19	2.55
Within Groups	14,212	55	258		
Total	15,441	59			

*Values have been truncated.

Result: $F_{.05,4,55} = 2.55 > 1.19$; the computed F value does not exceed the table value of F at the 5% level, indicating no significant difference between the means of the sets compared. Null hypothesis cannot be rejected.

TABLE XIV

T Test
(Comparing 80-cycle group with each other group)

X_1	T Value
No Prestress	3.21
Comp. Prestress	3.72
10 Cycle	4.06
20 Cycle	2.90
40 Cycle	3.97

Result: the table value ($T_{.01,23} = 2.81$) is smaller than the computed values of t in each case at the 1% confidence level, indicating a significant difference between the mean of the 80-cycle set and the means of all other sets. The null hypothesis of equal means must be rejected.

TABLE XV

Nonparametric U Test

(Mann - Whitney)

Sets Being Compared	Z Value
a) 40-cycle & 80-cycle	- 3.13
b) 20-cycle & 40-cycle	0.98

Result: a) $Z_{.01} = -2.33 > -3.13$

b) $Z_{.05} = 1.645 > 0.98$

The Z value obtained in the comparison of the 40-cycle and 80-cycle sets exceeds the table value of Z at the 1% level of significance. The null hypothesis of identical parent distribution must be rejected. In comparing the 20-cycle and 40-cycle sets, no significant difference is found at the 5% level.

APPENDIX C

THEORETICAL ANALYSIS OF THE EFFECT OF SPECIMEN ELLIPTICITY ON TENSILE STRENGTH

by

D. P. H. Hasselman and R. Sedlacek

Preceding Page Blank

Figure 16 is a schematic diagram of a thin-walled elliptical ring of unit length with the major axis of the elliptical cross section equal to a, and the minor axis equal to b. On internal pressurization, maximum bending moments will occur at the ends of the major axis (points A in Fig. 16 .) as shown in the work of Mayer-Mita[15] and Timoshenko;[16] maximum bending stresses are expected to occur at these points.

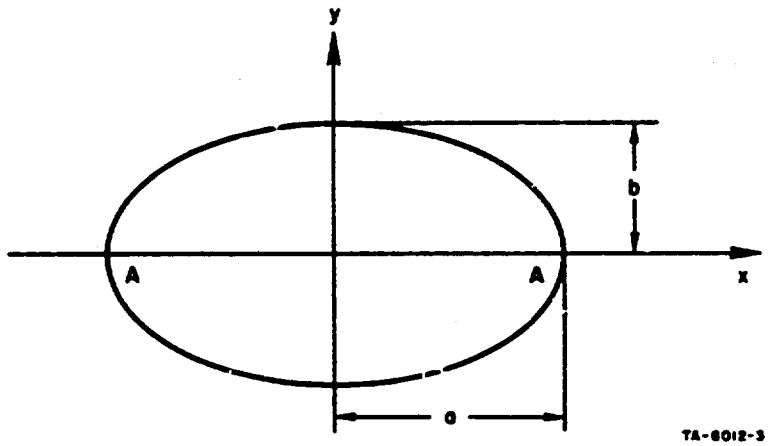

FIG. 16 CROSS SECTION OF INTERNALLY PRESSURIZED THIN ELLIPTICAL TUBE

The general approach taken in the present analysis is to consider the bending moments at points A and the resulting change in curvature due to these bending moments. With the known relationship for a bending moment as a function of pressure and given ellipticity, a differential equation is obtained relating the incremental change in bending moment to the increasing pressure and decreasing curvature. Solution of the differential equation results in the general expression for the bending moment as a function of internal pressure and initial

ellipticity of the specimen. The boundary conditions are determined by the original ellipticity of the unstressed ring and the final curvature of the pressurized ring which can be no less than that of a circle whose circumference is identical to that of the ellipse. The strains in the ring wall are assumed small in comparison with the size of the ellipse, so that changes in size to a first approximation can be neglected. The assumption is made that the shape of the ring retains the general shape of an ellipse during pressurization.

The general expression for the ellipse shown in Figure 16 at any time during pressurization can be written:

$$\frac{x^2}{a^2} + \frac{y^2}{b^2} = 1 \quad . \tag{C-1}$$

The general expression for the curvature (K) at any point on the circumference of the ellipse can be written:[18]

$$K = \frac{b}{a^2\left\{1 - \left(\frac{a^2 - b^2}{a^4}\right) x^2\right\}^{3/2}} \tag{C-2}$$

This expression for curvature also defines the size and shape of the ellipse at any time during its deformation. Thus, the displacements of the circumference of the ellipse are known at all times, which removes the statically indeterminate character of the problem.

The curvature (K_1) at point A can be computed to be

$$K_1 = a/b^2 \quad . \tag{C-3}$$

The curvature (K_2) of a circle with circumference equal to the circumference of the ellipse, with $C = 2\pi[(a^2 + b^2)/2]^{1/2}$, is

$$K_2 = [2/(a^2 + b^2)]^{1/2} \quad . \tag{C-4}$$

At any pressure P the difference (ΔK) between the curvature of the ellipse at point A and the curvature of a perfect circle can be written:

$$\Delta K = a/b^2 - [2/(a^2 + b^2)]^{1/2} \quad . \qquad \text{(C-5)}$$

The minor axis b can be expressed in terms of the out-of-roundness (ϵ) by:

$$b = a(1 - \epsilon), \quad \epsilon \ll 1, \qquad \text{(C-6)}$$

with the degree of out-of-roundness defined by

$$\epsilon = 1 - b/a \ . \qquad \text{(C-7)}$$

By substituting b of eq. (C-5) in eq. (C-6) and by using the approximations $(1 - 2\epsilon)^{-1} \approx 1 + 2\epsilon$ and $(1 - \epsilon)^{1/2} \approx 1 + \epsilon/2$ for $\epsilon \ll 1$, the difference (ΔK) by which the curvature of the ellipse differs from the curvature of the perfect circle becomes

$$\Delta K = -3\epsilon/2a \ . \qquad \text{(C-8)}$$

The bending moment (M) per unit length of ring, required to produce this curvature change, using the straight-beam approximation,[10*] given by

$$M(a) - M(\epsilon) = -EI\Delta K = 3EI\epsilon/2a \qquad \text{(C-9)}$$

where $M(\epsilon)$ is the bending moment at eccentricity (ϵ) and EI is the cross-sectional rigidity of short specimens, with E equal to Young's modulus of elasticity and I equal to the moment of inertia of the cross section per unit length. The moment of inertia per unit length is defined by $I = d^3/12$, where d is the ring wall thickness. Defining the ellipticity (ϵ) of the original unpressurized ring by $\epsilon = \epsilon_0$, we have $M(\epsilon_0) = 0$, and eq. (C-9) can be written:

$$M = (3EI/2a)(\epsilon_0 - \epsilon). \qquad \text{(C-10)}$$

An expression is now required for the change in bending moment with a change in pressure (dM/dP) for a given eccentricity. This information

* This approximation is valid for specimen wall thickness equal to or smaller than one-tenth the radius of curvature. To avoid excessive complexity, this approximation is assumed valid for all subsequent derivations.

can be obtained from the data of Mayer-Mita[15] shown in Fig. 17 which illustrates values of K in the expression $M = KPa^2$, for the maximum bending moment M in a rigid elliptical tube with internal pressure P and major axis equal to a. For values of $\epsilon < 0.02$, the results in Fig. 17 can be written to a very good approximation:

$$M = 0.5\,\epsilon\,Pa^2 \quad . \tag{C-11}$$

This yields, upon differentiation,

$$\frac{dM}{dP} = 0.5\,\epsilon\,a^2 \quad . \tag{C-12}$$

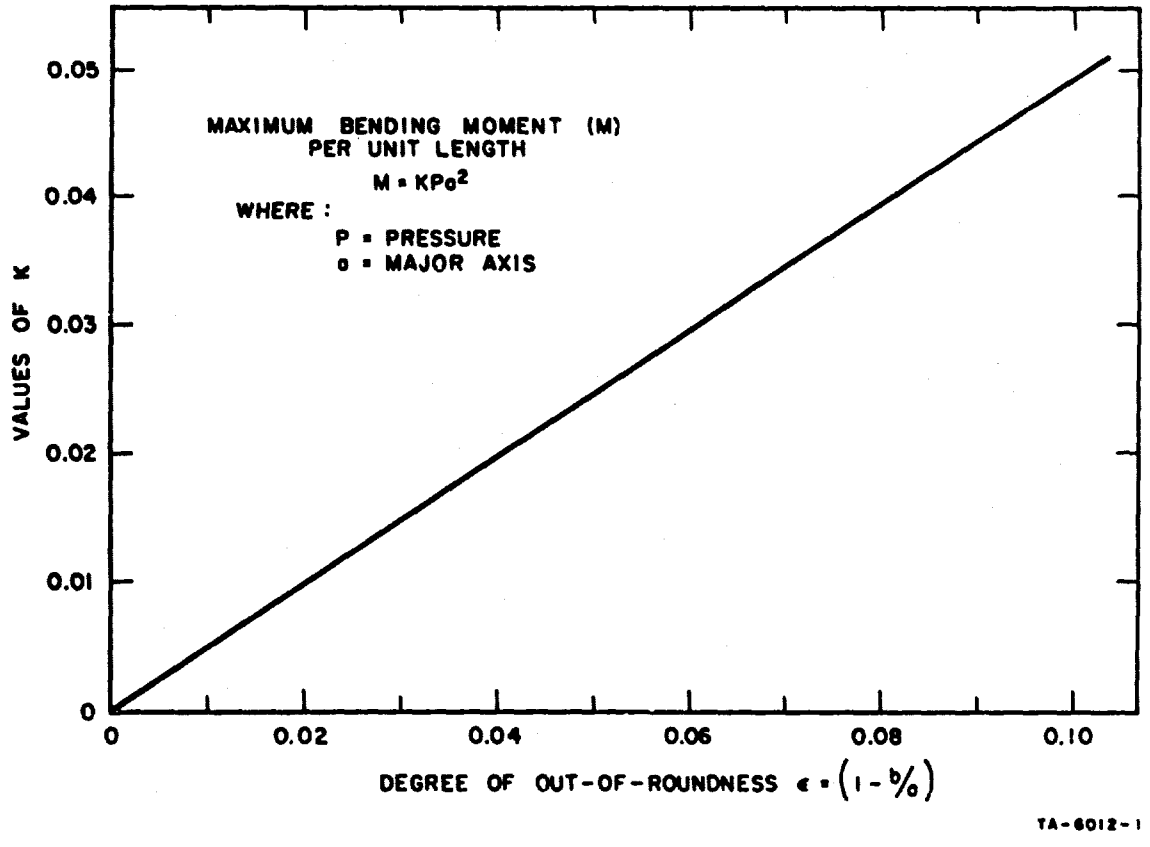

FIG. 17 BENDING MOMENTS IN INTERNALLY PRESSURIZED RIGID ELLIPTICAL TUBES

Substitution of eq. (C-12) for ϵ in eq. (C-10) and rearranging terms results in the differential equation

$$\frac{dM}{dP} + \frac{a^3 M}{3EI} = 0.5\epsilon_0 a^2 \qquad \text{(C-13)}$$

with solution[19]

$$M = \frac{3EI\epsilon_0}{2a}\left\{1-\exp[-a^3P/3EI]\right\}, \qquad \text{(C-14)}$$

which is the final expression desired.

Equation (C-14) indicates that the bending moment at point A (Fig. 16) rises asymptotically with increasing pressure to a constant value. This constant value of bending moment corresponds to the bending moment attained when the shape of the ellipse becomes circular. At low values of pressure or high values of cross-sectional rigidity, eq. (C-14) approaches the Mita-Timoshenko results (eq. C-11), which may be examined by letting, in eq.(C-14), $P \to 0$ or $EI \to \infty$. The quantity $\exp[-a^3P/3EI]$ then approximates $(1 - a^3P/3EI)$, which upon substitution in eq. (C-14) results in eq. (C-11). Eq. (C-14) also indicates that the bending moment is directly proportional to the original out-of-roundness of the unstressed ring. In the derivation of eq. (C-14), the decrease in length of the major axis with increasing pressure was not taken into account. It is easily shown that this introduces a maximum relative error in bending moment equal to one-half the degree of out-of-roundness, which for the present analysis can be neglected. Inclusion of changes of the major axis are easily incorporated in the derivation, but the results are nonlinear differential equations requiring lengthy numerical solutions.

Figure 18 illustrates the values of bending moment per unit length per 0.1 percent out-of-roundness for various values of cross-sectional rigidity (EI) for ring specimens whose nominal radii equal one inch. The curve for these values of cross-sectional rigidity corresponds to specimens whose wall thicknesses and values of Young's modulus of elasticity are occasionally encountered in the testing laboratory.

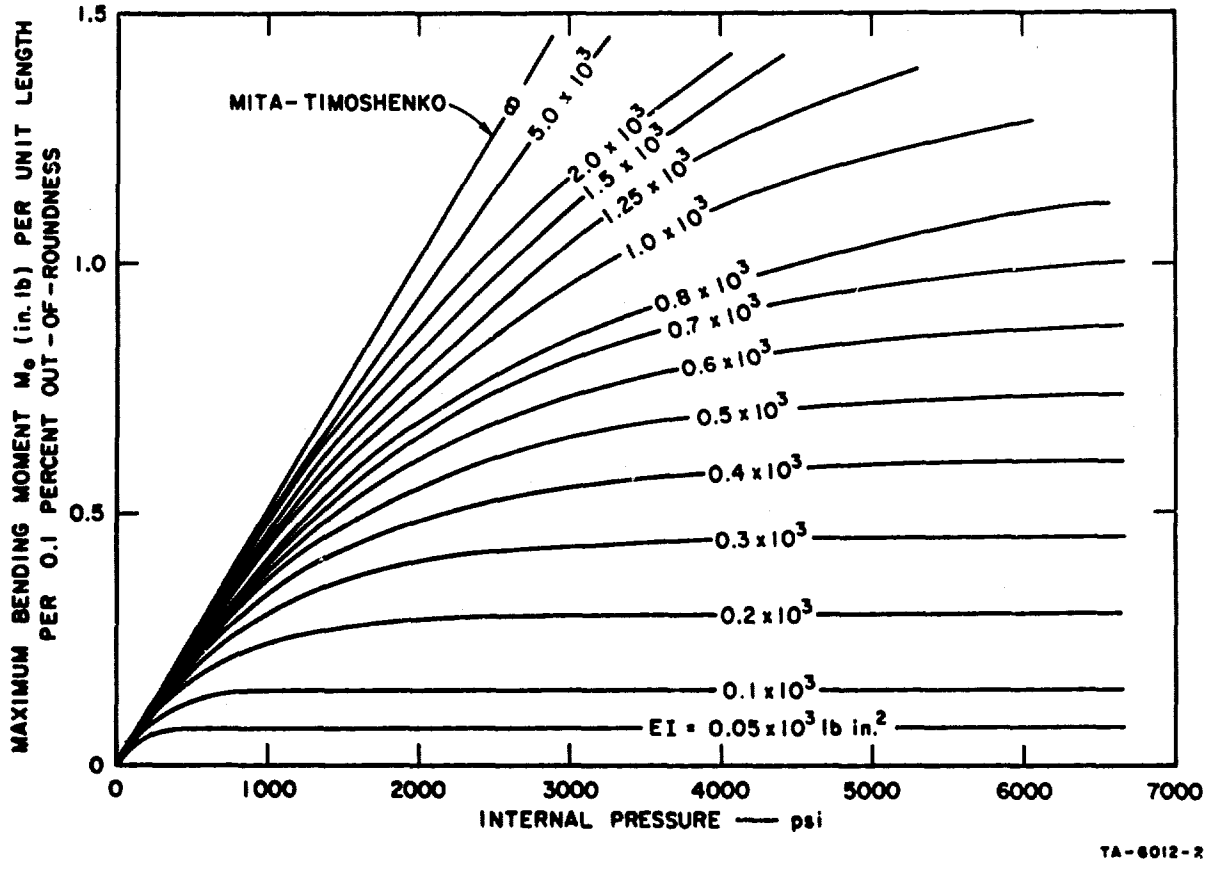

FIG. 18 BENDING MOMENTS IN INTERNALLY PRESSURIZED NONRIGID ELLIPTICAL TUBES

The curve for EI = ∞ corresponds to the Mita-Timoshenko analysis for rigid tubes. It is readily seen that the Mita-Timoshenko results usually overestimate the bending moments by an appreciable amount.

As a numerical example, additional stresses induced by the bending moments were calculated for ring specimens which had nominal diameters of one and two inches and out-of-roundness of $\epsilon_0 = 5 \times 10^{-4}$, a value to be expected in practice. Values of the wall thicknesses selected also correspond to those encountered in practice. Stresses were calculated for polycrystalline alumina, a relatively rigid material, and for graphite, a flexible material. The stresses were calculated at approximate pressure levels that would produce fracture. Table XVI shows the results obtained. For comparison, the stresses calculated using the Mita-Timoshenko analysis are also included. The stresses calculated using the present analysis are appreciably smaller.

TABLE XVI

CALCULATED BENDING STRESSES IN RING SPECIMENS HAVING AN OUT-OF-ROUNDNESS OF 0.05% AT APPROXIMATE PRESSURES REQUIRED TO CAUSE SPECIMEN FAILURE

Material	Wall Thickness (in.)	Specimen Diameter (in.)	Internal Pressure (psi)	Bending Stresses**	
				Present Analysis (psi)	Mita-Timoshenko (psi)
Al_2O_3*	0.1	1	6000	220	225
	0.1	2	3000	400	450
	0.05	1	3000	407	450
	0.05	2	1500	620	900
Graphite†	0.1	1	1000	31.6	37.5
	0.1	2	500	42.3	75
	0.05	1	500	12.9	75
	0.05	2	250	18.5	150

*Assumed: $E = 60 \times 10^6$ psi; tensile strength (S_t) = 30,000 psi.

†Assumed: $E = 1.5 \times 10^6$ psi; tensile strength (S_t) = 5000 psi.

**Calculated from $S = Md/2I$.

In general, the smaller the ring size the smaller are the resulting bending stresses. For the one-inch alumina rings the bending stresses are of the order of approximately one percent of the value of strength, whereas for the graphite specimens the bending stresses amount to approximately one-half percent or less. For the two-inch diameter rings these percentages are approximately doubled. For the value of out-of-roundness assumed for the data in Table XVI $\epsilon_0 = 5 \times 10^{-4}$, the relative effect of bending stresses is similar to or less than the generally observed scatter in strength values. For this value of out-of-roundness the effect of specimen eccentricity on the value of fracture strength may be neglected.

Of exceptional interest is the effect of specimen wall thickness on the bending stresses in graphite specimens as compared with alumina specimens. Decreasing the wall thickness increases the induced bending

stresses in alumina, as calculated on the basis of the present derivation and the Mita-Timoshenko analysis. For graphite specimens, however, the bending stresses are reduced on decreasing the wall thickness using the present analytical method; whereas, the Mita-Timoshenko analysis, which predicts a bending moment independent of wall thickness, results in an increase in bending stresses for graphite. These opposite effects occur because the values of cross-sectional rigidity for the graphite specimens are much lower than the corresponding values for alumina specimens. In terms of eq. (C-14), for the graphite specimens a decrease in the cross-sectional rigidity (EI) causes a much greater decrease in final bending moment than the corresponding increase in bending stress with decreasing wall thickness for a given value of (M). For the alumina specimens, however, the effect of decreasing the value of cross-sectional rigidity (EI) on the final bending moment (M) is relatively small resulting in an increase in bending stress.

From the point of view of the size of the specimen for the present program, the wall thickness selected represents a near-optimum for minimizing the effect of specimen ellipticity, while maintaining a high stress uniformity within the specimen.

During the experimental determination of tensile strength, the point of failure of a slightly elliptical specimen may not always coincide with the point where the bending stresses are a maximum, because of the statistical nature of brittle fracture. For a detailed calculation of strength, the value of bending moment at the point of failure is of interest rather than the maximum bending moment at the end of the major axis. This value of bending moment for nearly circular rings to a very good approximation can be expressed by:

$$M_{\alpha} = M_0 \cos 2\alpha \qquad \text{(C-15)}$$

where M_{α} is the bending moment at the point of failure, M_0 is the maximum bending moment (eq. (C-14)), and α is the angle between the point of failure and the point of maximum bending moment (end of major axis).

The total stress (S) that occurs in the ring is composed of the bending stresses superposed on the uniform stresses and can be expressed by

1. Exact equation:

$$S = P(r_o^2 + r_i^2)/(r_o^2 - r_i^2) + \frac{3E\epsilon_0 d}{2D}\left[1 - \exp\left\{-a^3P/3EI\right\}\right]\cos 2\alpha \qquad \text{(C-16)}$$

2. Thin-tube approximation:

$$S = PD/2d + \frac{3E\epsilon_0 d}{2D}\left[1 - \exp\left\{-a^3P/3EI\right\}\right]\cos 2\alpha \qquad \text{(C-17)}$$

where r_o and r_i are the nominal outside and inside radii of the ring, respectively, and D is the nominal diameter with $D = 2a$, and with $a = (r_o + r_i)/2$. The second term on the right side of eqs. (C-16) and (C-17) was obtained by means of eq. (C-15) and the relation between maximum bending stress (S_b) and bending moment (M) expressed by: $S_b = Md/2I$. For very precise stress calculations the nominal specimen dimensions can be replaced by the actual specimen dimensions measured at the maximum diameter.

TABLE XVII

TENSILE STRENGTH OF ROUND AND ELLIPTICAL PLEXIGLAS SPECIMENS
(Stress Rate $\dot{\sigma}$ = 5000 psi/sec)

Specimen Number	Ellipticity (%)	Ultimate Tensile Strength (psi)	Deviation (psi)
1	0	14,370*	
2	0	14,670	-710
3	0	15,010	-370
4	0	15,430	+ 50
5	0	15,320	- 60
6	0	16,180	+800
7	0	15,390	+ 10
8	0	15,470	+ 90
9	0	15,840	+460
10	0	15,130	-250
Average	0	15,380	±420 (2.7%)
1	1	14,040	-1690
2	1	16,120	+390
3	1	16,300	+570
4	1	16,320	+590
5	1	15,550	-180
6	1	15,260	-470
7	1	15,590	-140
8	1	15,490	-240
9	1	16,520	+790
10	1	16,150	+420
Average	1	15,730	±690 (4.4%)

* Hydrostatic pressure was programmed too low and specimen No. 1 failed after 0.25 sec at the stress indicated.

TABLE XVII (Continued)

Specimen Number	Ellipticity (%)	Ultimate Tensile Strength (psi)	Deviation (psi)
1	2	16,000	+160
2	2	15,530	-310
3	2	16,380	+540
4	2	16,140	+300
5	2	15,360	-480
6	2	16,160	+320
7	2	15,830	- 10
8	2	16,300	+460
9	2	15,480	-360
10	2	15,190	-650
Average	2	15,840	±400 (2.5%)
1	3	13,860	-1870
2	3	15,650	- 80
3	3	15,560	-170
4	3	15,830	+100
5	3	15,830	+100
6	3	16,240	+310
7	3	16,040	+210
8	3	16,330	+600
9	3	15,860	+130
10	3	16,140	+410
Average	3	15,730	±660 (4.2%)

TABLE XVII (Concluded)

Specimen Number	Ellipticity (%)	Ultimate Tensile Strength (psi)	Deviation (psi)
1	4	15,920	+ 60
2	4	16,300	+440
3	4	16,110	+250
4	4	16,200	+340
5	4	15,530	-370
6	4	16,200	+340
7	4	15,530	-330
8	4	15,500	-310
9	4	15,800	- 60
10	4	15,470	-390
Average	4	15,860	±310 (2.0%)
1	5	15,310	- 10
2	5	14,090	-1230
3	5	14,880	-440
4	5	15,650	+330
5	5	15,710	+390
6	5	15,580	+260
7	5	15,990	+670
8	5	16,020	+700
9	5	14,780	-540
10	5	15,220	-100
Average	5	15,320	±570 (3.7%)

TABLE XVIII

TENSILE STRENGTH OF ROUND AND ELLIPTICAL PLEXIGLAS SPECIMENS
(Stress Rate $\dot{\sigma}$ = 50,000 psi/sec)

Specimen Number	Ellipticity (%)	Ultimate Tensile Strength (psi)	Deviation (psi)
1	0	17,290	+780
2	0	16,080	-430
3	0	15,530	-980
4	0	16,360	-150
5	0	17,280	+770
Average	0	16,510	±690 (4.2%)
1	3	16,640	-140
2	3	16,450	-330
3	3	16,910	+130
4	3	16,900	+120
5	3	17,000	+220
Average	3	16,780	±200 (1.2%)
1	5	16,230	-380
2	5	16,900	+290
3	5	17,040	+430
4	5	16,230	+380
5	5	16,640	+ 30
Average	5	16,610	±330 (2.0%)

TABLE XIX

TENSILE STRENGTH OF ROUND AND ELLIPTICAL ATJ GRAPHITE SPECIMENS
(Stress Rate $\dot{\sigma}$ = 50,000 psi/sec)

Specimen Number	Ellipticity (%)	Ultimate Tensile Strength (psi)	Deviation (psi)
1	0	3890	-110
2	0	4220	+220
3	0	4060	+ 60
4	0	4230	+230
5	0	3650	-350
6	0	3860	-140
7	0	4190	+190
8	0	3860	-140
Average	0	4000	±200 (5.0%)
1	5	2810	-210
2	5	3230	+210
3	5	3030	+ 10
4	5	2940	- 80
5	5	2930	- 90
6	5	3210	+190
7	5	2960	- 60
8	5	3080	+ 60
Average	5	3020	±140 (4.5%)

ACKNOWLEDGMENT

The author wishes to express his appreciation to Mr. H. Stuart Starrett of the Southern Research Institute who conducted the study of the flexural strength of alumina.

REFERENCES

1. Pears, C. D., Evaluation of Tensile Data for Brittle Materials Obtained with Gas Bearing Concentricity, Technical Documentary Report No. ASD-TDR-63-245, May 1963.

2. Sedlacek, R., and F. A. Halden, "Method for Tensile Testing of Brittle Materials," Rev. Sci. Instr., 33, 298-300 (1962).

3. Sedlacek, R., Tensile Strength of Brittle Materials, Technical Documentary Report No. ML-TDR-64-49, Air Force Materials Laboratory, Wright-Patterson Air Force Base, Ohio, March 1964.

4. Sedlacek, R., Tensile Strength of Brittle Materials, Technical Report AFML-TR-65-129, Air Force Materials Laboratory, Wright-Patterson Air Force Base, Ohio, August 1965.

5. Bortz, S. A., and T. Wade, Analysis of Mechanical Testing Procedure for Brittle Materials, AMRA CR 67-0911 Interim Report, September 1967.

6. Sedlacek, R., and E. P. Farley, Processing of Ceramics--Surface Finishing Studies, Prepared under Contract No. NOw 66-0383-d for the Naval Air Systems Command, May 1967.

7. Sedlacek, R., Tensile Fatigue Strength of Brittle Materials, Technical Report AFML-TR-66-245, Air Force Materials Laboratory, Wright-Patterson Air Force Base, Ohio, March 1968.

8. Sedlacek, R., Comparison of Elastic Properties of Ceramics under Compressive and Tensile Stress, SRI Project 184531-122, May 1965.

9. Moberly, J. W., et al., "Hydrostatic Ring Test for High Precision Strain Measurements," Rev. Sci. Instr., 39, 835-837 (1968).

10. Roark, R. J., Formulas for Stress and Strain, 4th Ed., McGraw-Hill Book Company, New York, 1965.

11. Prosen, S. P., A Method of Test for Determining the Compressive Properties of Filament Wound NOL Rings, Technical Report NOLTR 64-80, United States Naval Ordnance Laboratory, White Oak, Maryland, July 1964.

12. Weil, N. A., Studies of the Brittle Behavior of Ceramic Materials, ARF Report No. 8203-18 (Quarterly Report), Contract No. AF 33(616)-7465, May 1962.

13. Neuber, H., and A. Wimmer, Experimental Investigations of the Behavior of Brittle Materials at Various Ranges of Temperature, Technical Report AFML-TR-68-23, Air Force Materials Laboratory, Wright-Patterson Air Force Base, Ohio, March 1968.

14. Rudnick, A., et al., The Evaluation and Interpretation of Mechanical Properties of Brittle Materials, Technical Report AFML-TR-67-361, DCIC Report 68-3, Wright-Patterson Air Force Base, Ohio, April 1968.

REFERENCES (Concluded)

15. Mayer-Mita, R., "Die Berechnung dünnwandiger ovaler (im besonderen elliptischer) Röhren gegen gleichformigen Normaldruck," Z. Ver. Deut. Ing., 17, 649-654 (1914).

16. Timoshenko, S., Strength of Materials, Part I, 3rd ed., pp. 389-390, D. van Nostrand Company, 1955.

17. Warden, C. J., and S. J. Green, Response of Materials and Structures to Suddenly Applied Stress Loads: Phase I, General Motors Defense Research Laboratories Report TR-65-69, October 1965.

18. Wylie, C. R., Advanced Engineering Mathematics, p. 629, McGraw-Hill Book Company, New York, 1951.

19. Reddick, H. W., and F. H. Miller, Advanced Mathematics for Engineers, 3rd ed., p. 13, John Wiley and Sons, New York, 1955.

Unclassified
Security Classification

DOCUMENT CONTROL DATA - R & D

(Security classification of title, body of abstract and indexing annotation must be entered when the overall report is classified)

1. ORIGINATING ACTIVITY (Corporate author) Stanford Research Institute 333 Ravenswood Avenue Menlo Park, California 94025	2a. REPORT SECURITY CLASSIFICATION Unclassified 2b. GROUP

3. REPORT TITLE

INVESTIGATION OF ELASTICITY AND STRENGTH OF CERAMICS SUBJECTED TO TENSILE AND COMPRESSIVE LOADS

4. DESCRIPTIVE NOTES (Type of report and inclusive dates)

Final Report 15 April 1966 to 31 May 1968

5. AUTHOR(S) (First name, middle initial, last name)

Rudolf Sedlacek

6. REPORT DATE	7a. TOTAL NO. OF PAGES	7b. NO. OF REFS
February 1969	93	19

8a. CONTRACT OR GRANT NO. AF 33(615)-5047 b. PROJECT NO. 7350 c. TASK No. 735003 d.	9a. ORIGINATOR'S REPORT NUMBER(S) FMU-6012 9b. OTHER REPORT NO(S) (Any other numbers that may be assigned this report) AFML-TR-68-231

10. DISTRIBUTION STATEMENT This document is subject to special export controls and each transmittal to foreign governments or foreign nationals may be made only with prior approval of the Metals and Ceramics Division (MAM), Air Force Materials Laboratory, Wright-Patterson Air Force Base, Ohio 45433.

11. SUPPLEMENTARY NOTES	12. SPONSORING MILITARY ACTIVITY
	Air Force Materials Laboratory Air Force Systems Command Wright-Patterson Air Force Base, Ohio

13. ABSTRACT

A new method of compressive testing of ceramics was perfected, and the average ultimate compressive strength of Al-995 alumina was determined to be 448,000 ± 36,000 psi at a loading rate of 10,000 psi/sec. Compressive prestressing was found to have no significant effect on the ultimate tensile strength of alumina, but extensive cyclic testing did lower the ultimate tensile strength. A statistical evaluation of test data supported these experimental results. Compressive and tensile elastic moduli and Poisson's ratios were measured. Flexural strength was found to be slightly higher than tensile strength. A theoretical analysis and experimental study were made of the effect of out-of-roundness on the nominal tensile strength of internally pressurized cylindrical test specimens. It was found that the effect of out-of-roundness which is occasionally encountered in commercially fabricated ceramic specimens is small and well within the experimental data scatter.

This abstract is subject to special export controls and each transmittal to foreign governments or foreign nationals may be made only with prior approval of the Metals and Ceramics Division (MAM), Air Force Materials Laboratory, Wright-Patterson Air Force Base, Ohio 45433.

14 KEY WORDS	LINK A		LINK B		LINK C	
	ROLE	WT	ROLE	WT	ROLE	WT
ALUMINA						
COMPRESSIVE RING TEST						
TENSILE RING TEST						
COMPRESSIVE STRENGTH						
TENSILE STRENGTH						
EFFECT OF PRESTRESSING						
ELASTIC MODULUS						
POISSON'S RATIO						
EFFECT OF OUT-OF-ROUNDNESS						